SAND2017-2055C

Quantifying material variability and uncertainty for welded and additively-manufactured structures using multiscale a posteriori error-estimation techniques

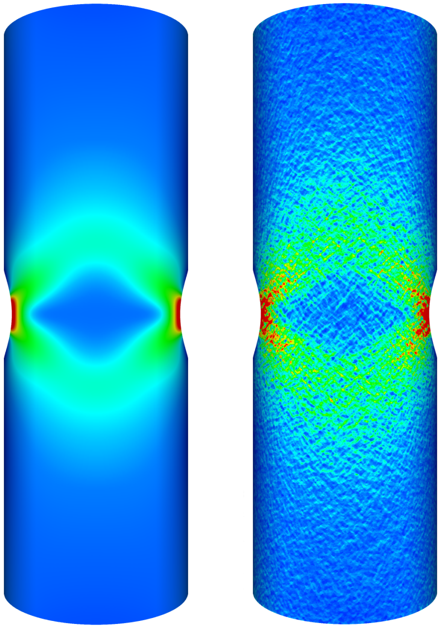

Joe Bishop, Judy Brown

Engineering Sciences Center

Sandia National Laboratories

Sandia National Laboratories

Exceptional service in the national interest

TMS 146th Annual Meeting & Exhibition
February 26 – March 2, 2017
San Diego, CA

U.S. DEPARTMENT OF ENERGY

NNSA National Nuclear Security Administration

Sandia National Laboratories is a multi-mission laboratory managed and operated by Sandia Corporation, a wholly owned subsidiary of Lockheed Martin Corporation, for the U.S. Department of Energy's National Nuclear Security Administration under contract DE-AC04-94AL85000.

Acknowledgements

Collaborators:

- Judy Brown
- Theron Rodgers
- Kyle Johnson
- Jon Madison
- John Emery
- David Littlewood
- Ben Reedlunn
- Corbett Battaile

Outline

1. engineering science questions
2. comparison of homogenization results and “direct numerical simulation” (DNS)
3. multi-scale error estimation and UQ
4. conclusions, future work

Science questions

1. Does a material "property" exist for metal AM (or welds)?
2. What are the errors in engineering quantities-of-interest in assuming homogeneous constitutive behavior?
3. How to do multiscale uncertainty quantification for metal AM and welded materials?

Multiscale UQ research theme

- Use a relatively simple model at the macroscale, but assess error *a posteriori* with respect to a more accurate “reference” model. (Oden, et.al. 1996-2004).
- This is a combination of aleatory and epistemic UQ.
- Need a “reference model” (or advanced experiments).
- Adapt macroscale model to reduce error or uncertainty.

Error estimation as UQ

variable microstructure

- simple macroscale model
- deterministic (simulate once)
- assess error *a posteriori*

variable geometry

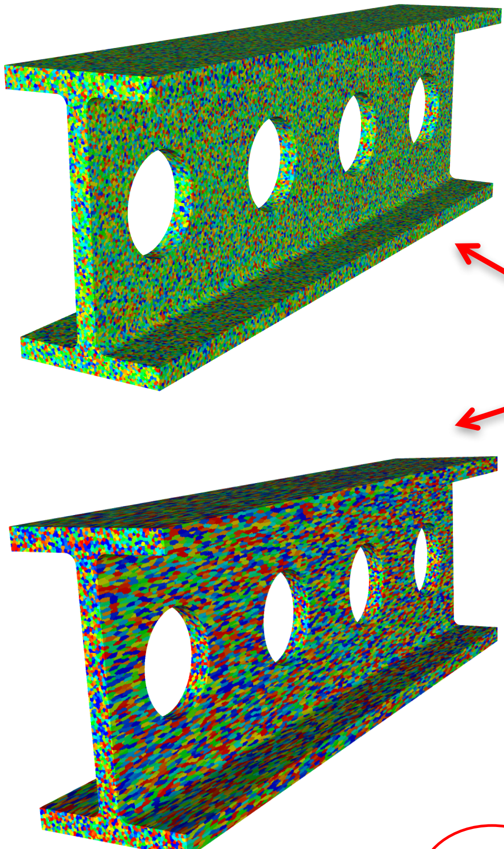

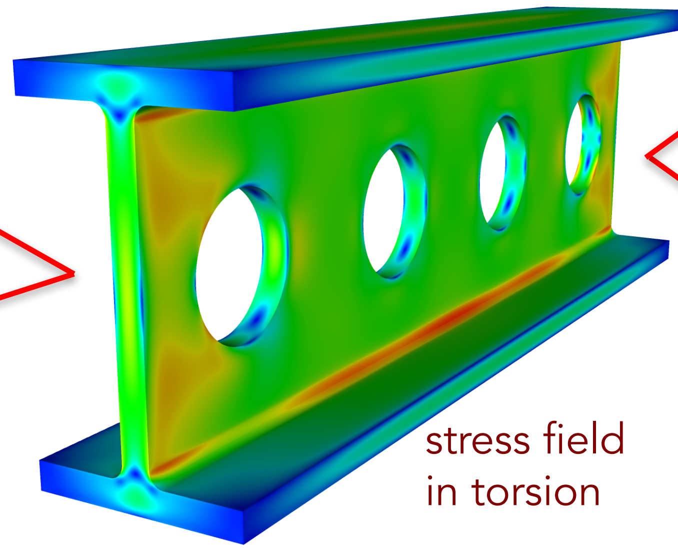

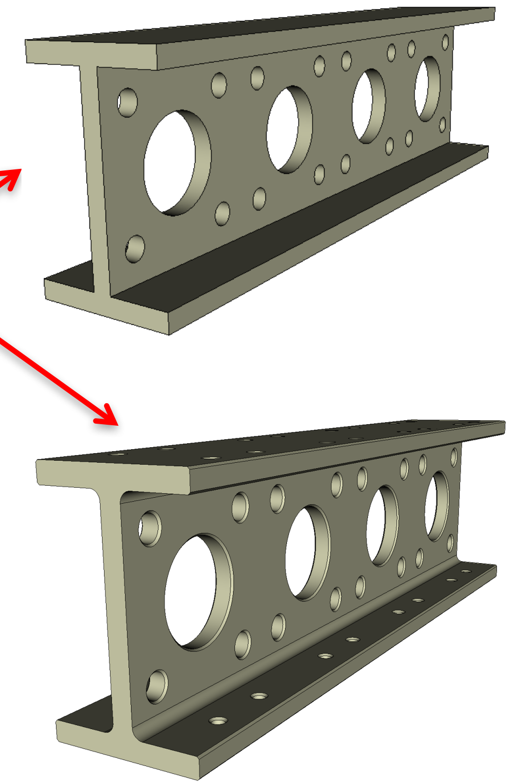

error bound (Oden, et. al., 1997)

$$\|\mathbf{u}(\omega) - \mathbf{u}^0\|_E^2 \leq \int_\Omega (\boldsymbol{\varepsilon}^0 - \bar{\boldsymbol{\varepsilon}}(\omega)) : (\bar{\boldsymbol{\sigma}}(\omega) - \boldsymbol{\sigma}^0)\, d\Omega$$

Error estimation and adaptivity

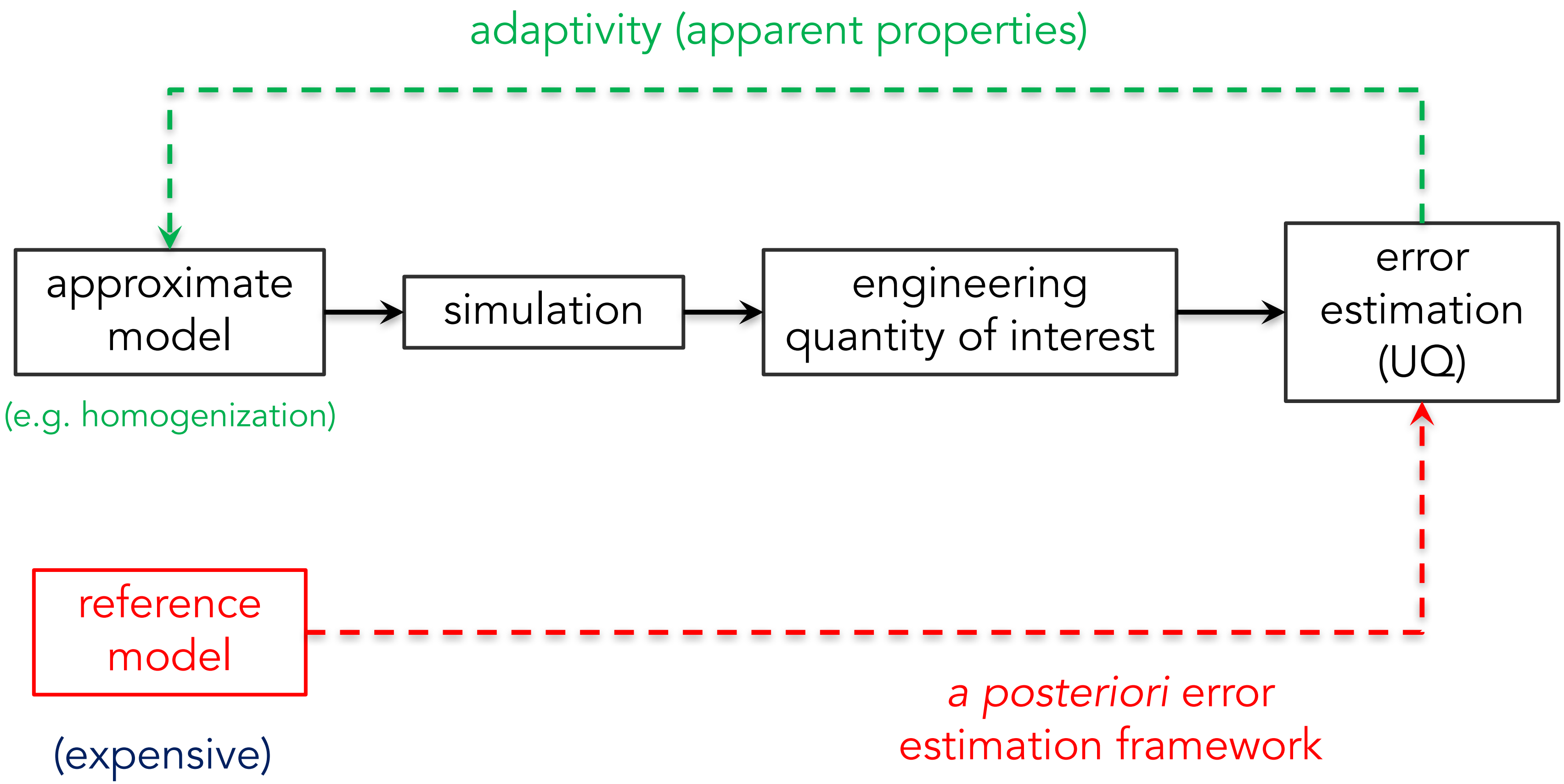

Laser weld EBSD, 304L

1 mm

welding direction

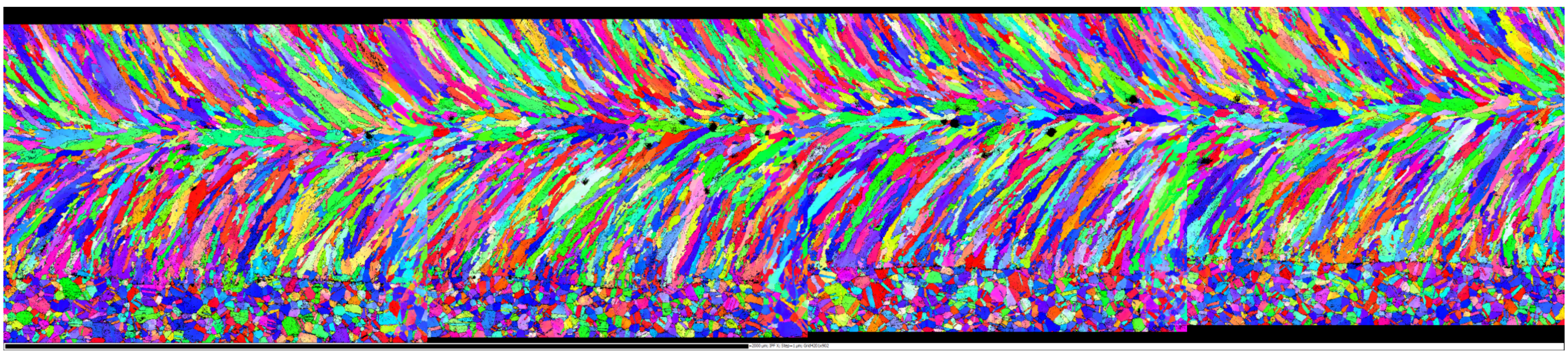

How to homogenize?

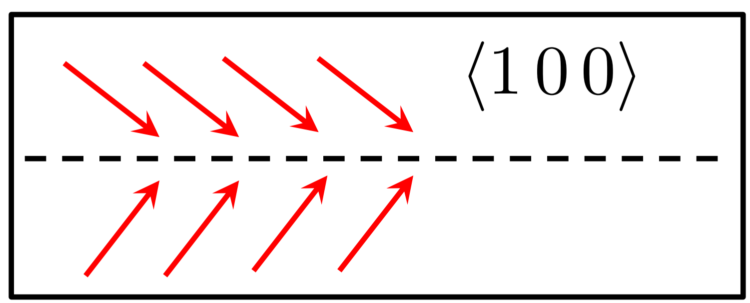

Effect of texture on homogenized elastic properties

austenite grain (FCC)
304L

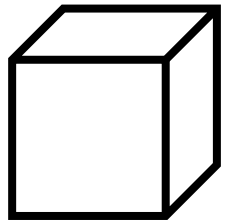

cubic symmetry (3 independent)

$$E = 93.8\ \text{GPa}$$
$$\nu = 0.402$$
$$G = 126\ \text{GPa}$$

no texture

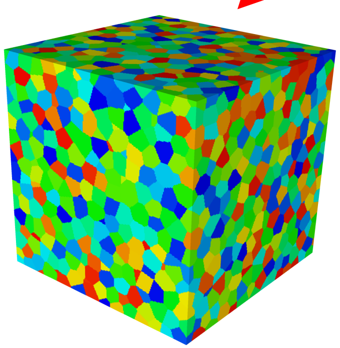

isotropic (2 independent)

$$E = 198\ \text{GPa}$$
$$\nu = 0.294$$
$$G = 76.5\ \text{GPa}$$

$$G = \frac{E}{2(1+\nu)}$$

ideal fiber-texture
along [001]

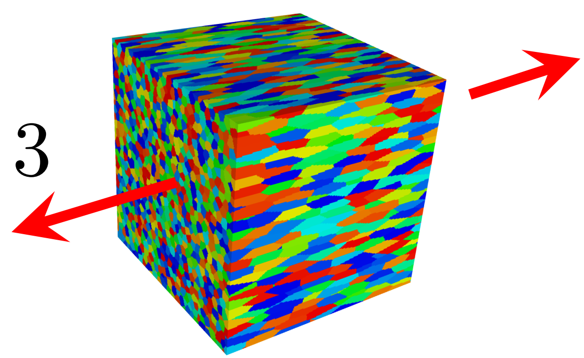

transversely isotropic

$$E_{11} = 143\ \text{GPa}$$
$$E_{22} = 143\ \text{GPa}$$
$$E_{33} = 90.9\ \text{GPa}$$
$$\nu_{12} = 0.114$$
$$\nu_{23} = 0.615$$
$$\nu_{13} = 0.615$$
$$G_{12} = 58\ \text{GPa}$$
$$G_{23} = 126\ \text{GPa}$$
$$G_{13} = 126\ \text{GPa}$$

LENS, Laser Engineered Net Shaping

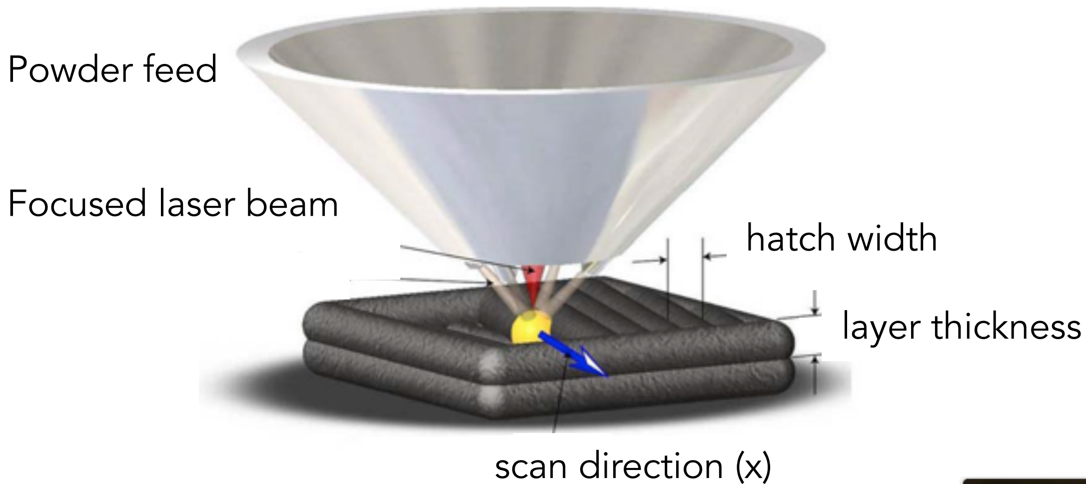

LENS deposition

(T. Palmer, PSU)

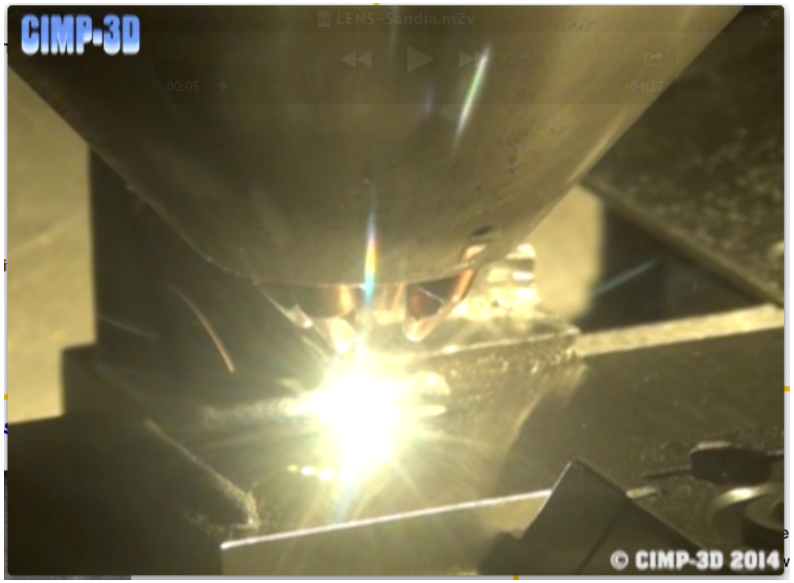

Microstructure comparison, 304L

Sandia National Laboratories

(D. Adams)

Wrought

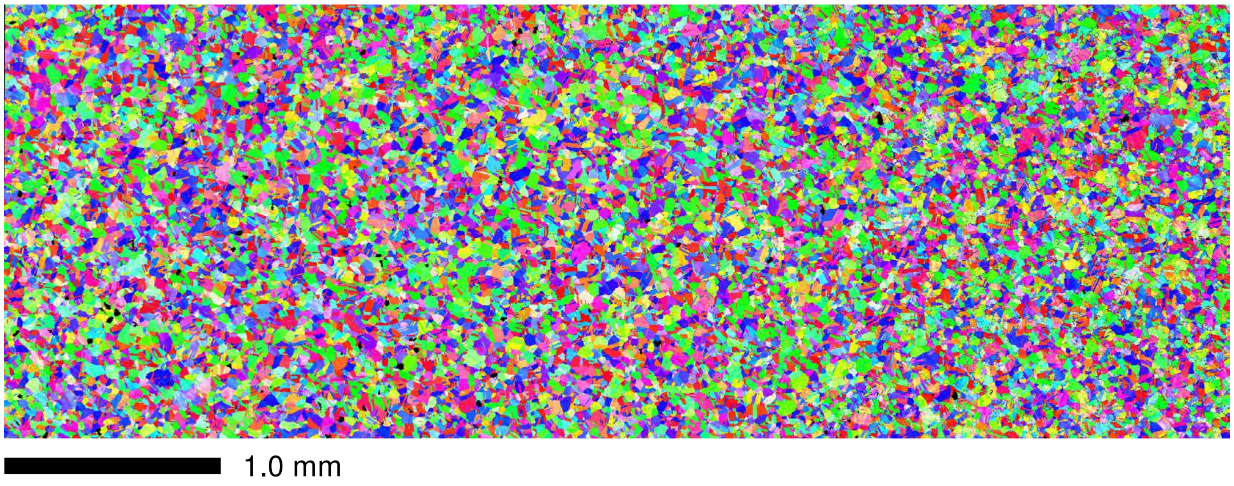

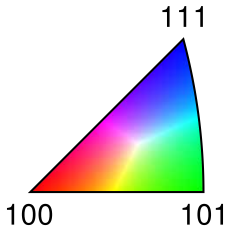

3.8 kW LENS

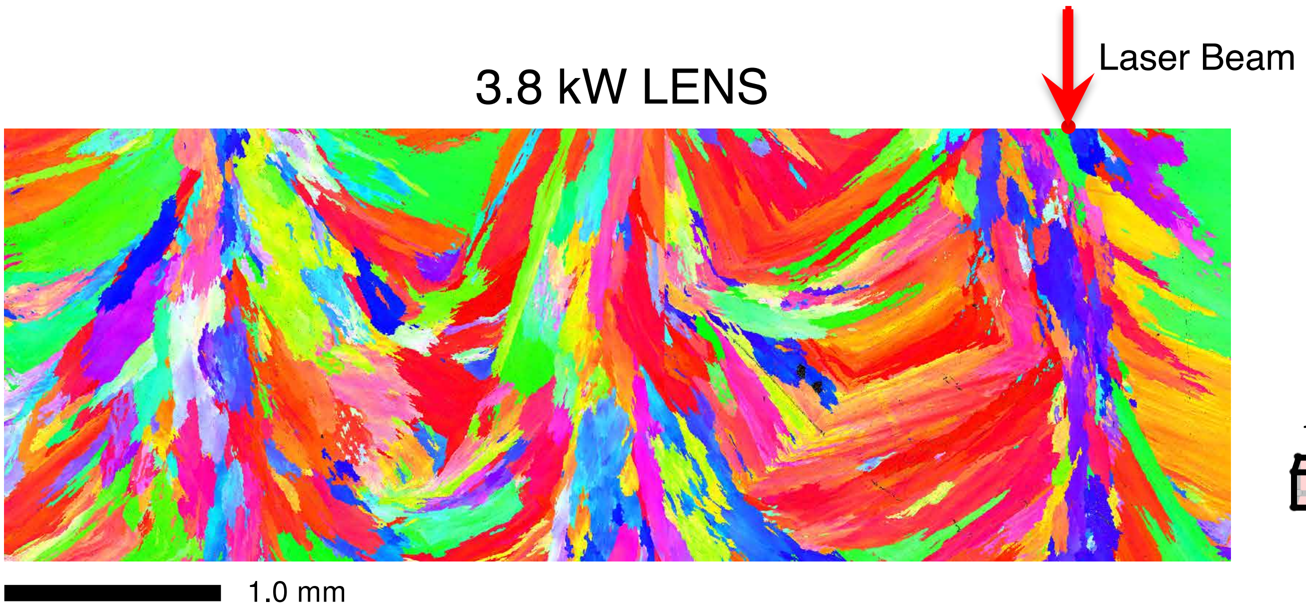

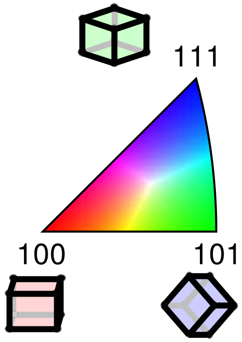

Example

Sandia National Laboratories

Consider two processing steps

1. AM build for tube (LENS, PB)
2. subtractive machining for side hole

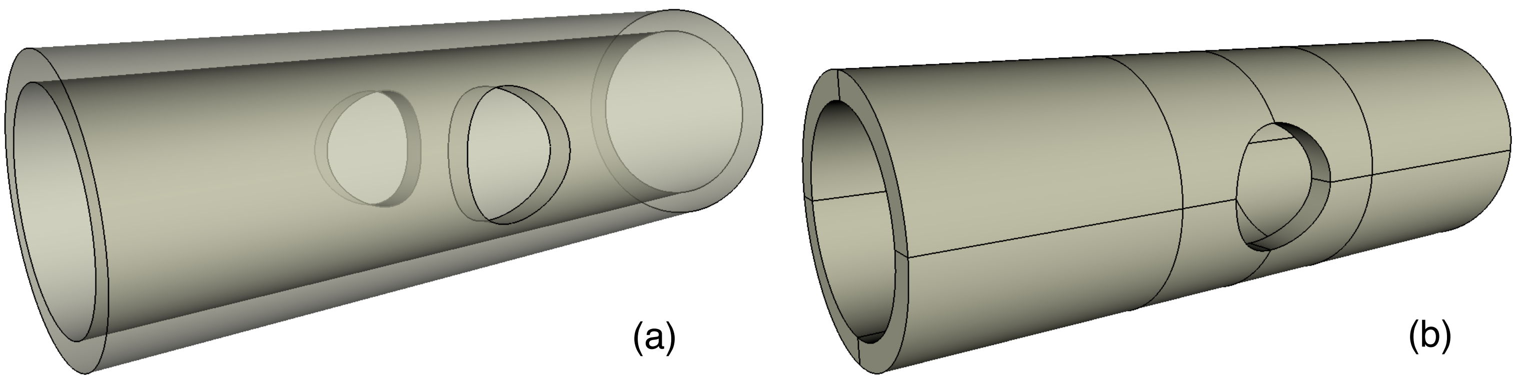

Consider two synthetic microstructures:

1. equiaxed (wrought)
2. additive (LENS using Kinetic Monte Carlo)

Microstructure generation

(T. Rodgers, V. Tikare, J. Madison) (spparks.sandia.gov)

- Kinetic Monte Carlo (KMC)
- Laser-welding simulation

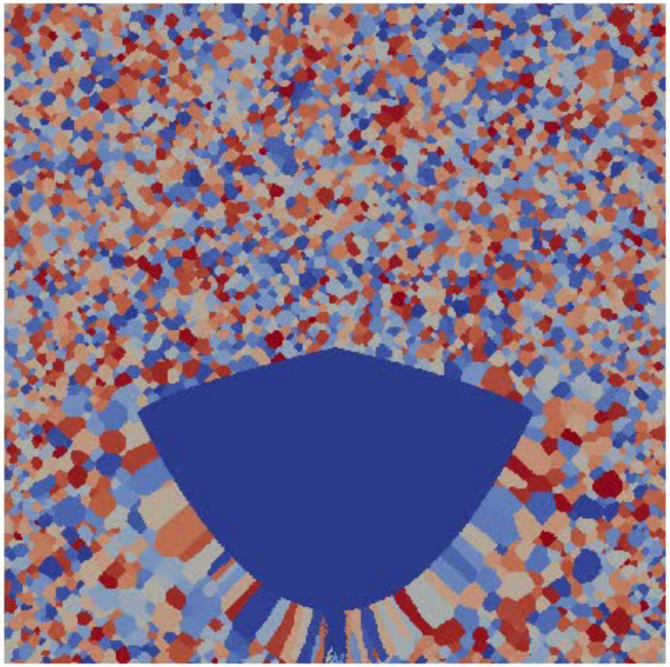

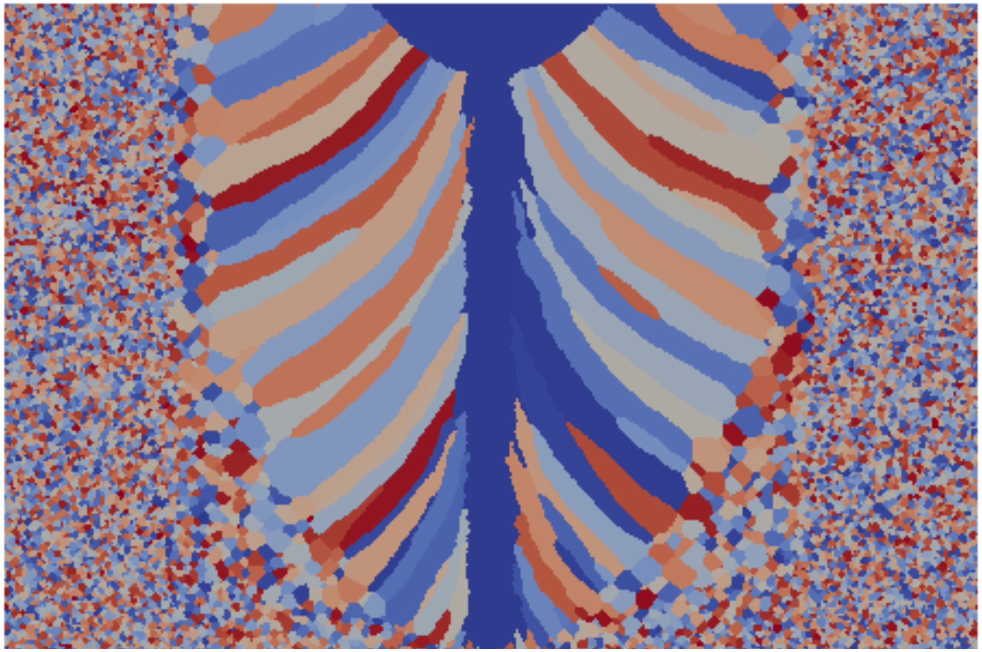

Synthetic additive microstructure using KMC

(Theron Rodgers)

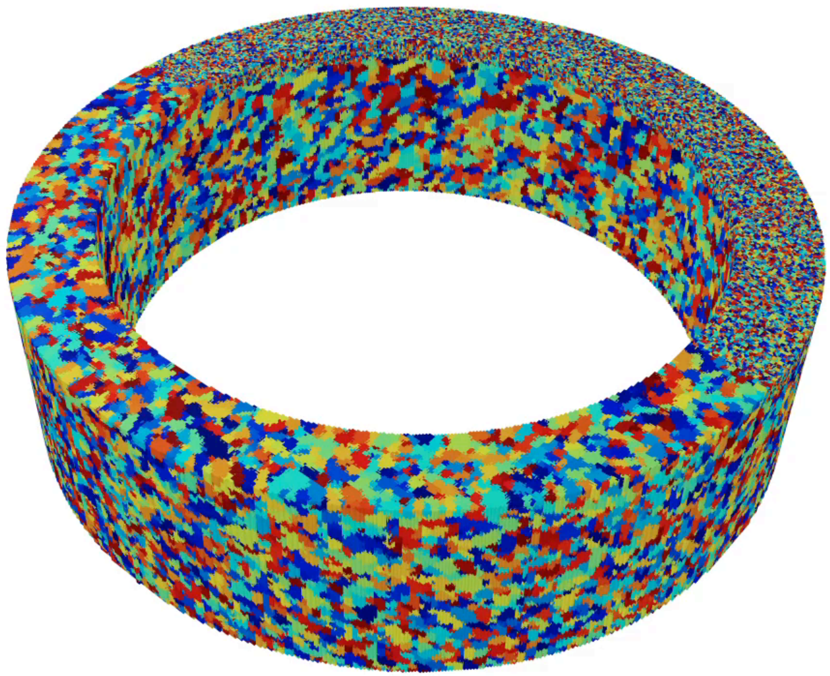

- KMC additive simulation
- single laser pass per layer
- 100 layers
- overlap with previous layer

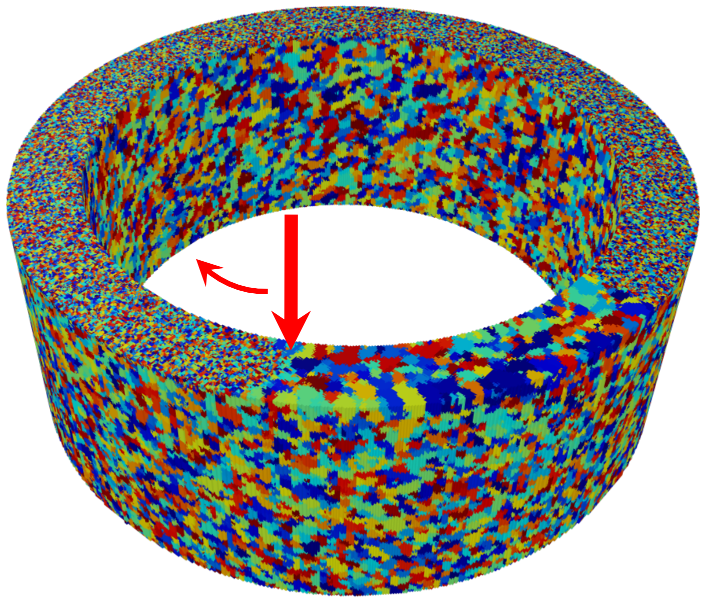

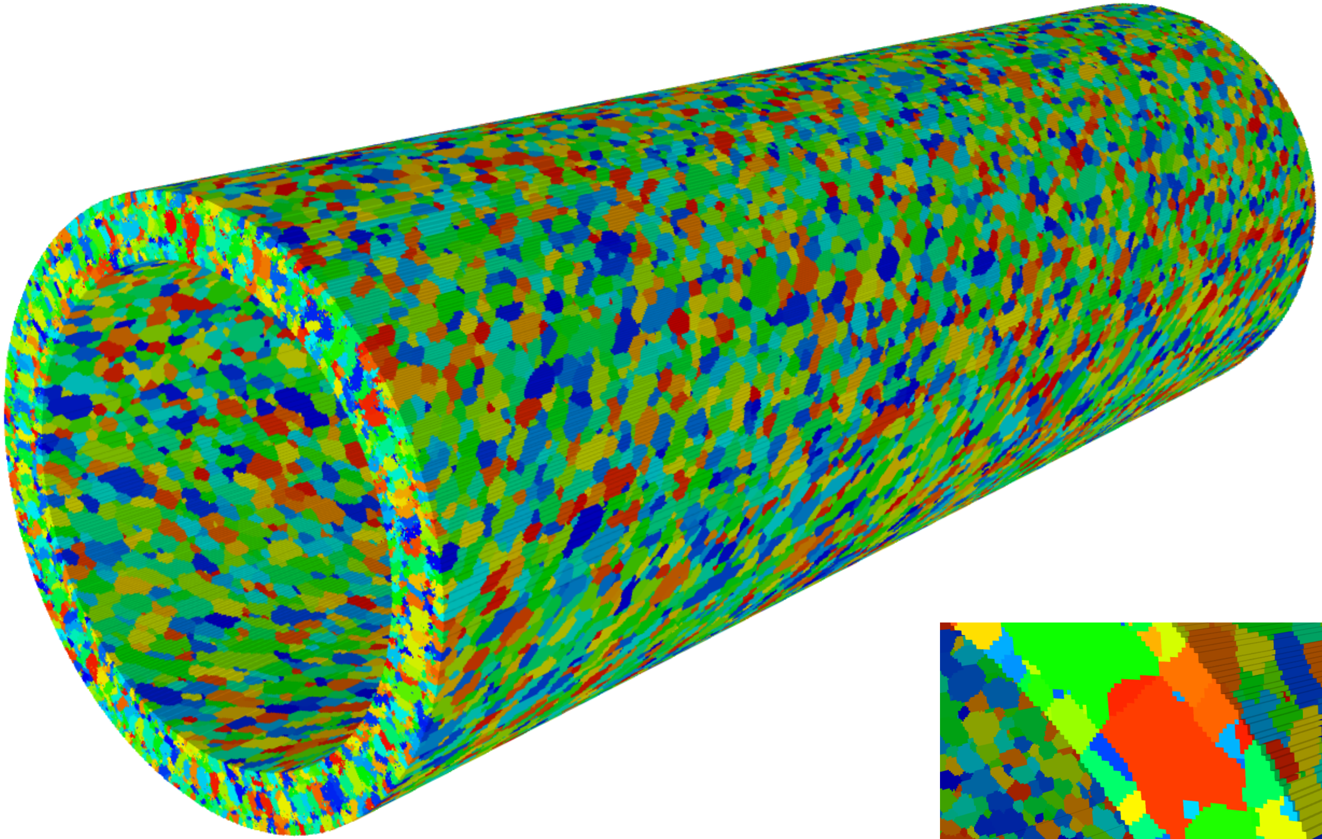

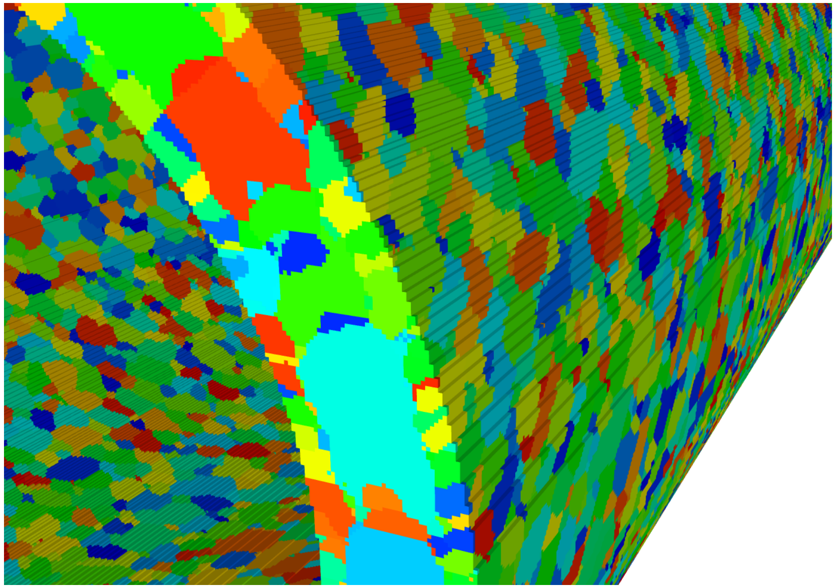

- KMC (SPPARKS) voxelated geometry
- 55M voxels
- two laser passes per layer (difference between surface and interior microstructure)

FCC crystal plasticity model

plastic velocity gradient: $$L^p = \sum_{\alpha=1}^{N} \dot{\gamma}^\alpha P^\alpha$$

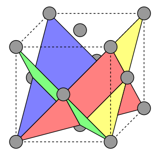

Schmid tensor: $$P^\alpha = m^\alpha \otimes n^\alpha$$

slip system slip rates: $$\dot{\gamma}^\alpha = \dot{\gamma}_0 \left(\frac{\tau^\alpha}{g}\right)^{1/m} \cdot \mathrm{sign}(\tau^\alpha)$$

slip system hardening: $$g = g_o + (g_{so} - g_o)\left[1 - \exp\left(-\frac{G_o}{g_{so} - g_o}\gamma\right)\right]$$

$$\gamma = \sum_{s=1}^{N} |\gamma^s|$$ (sum over slip systems)

Single crystal elastic constants (austenite)

$$C_{11} = 204.6 \text{ GPa}$$
$$C_{12} = 137.7 \text{ GPa}$$
$$C_{44} = 126.2 \text{ GPa}$$

Not considering:

- grain boundary effects (Hall-Petch effect)
- twinning
- dislocation substructures
- latent hardening

Representative Volume Element (RVE) response

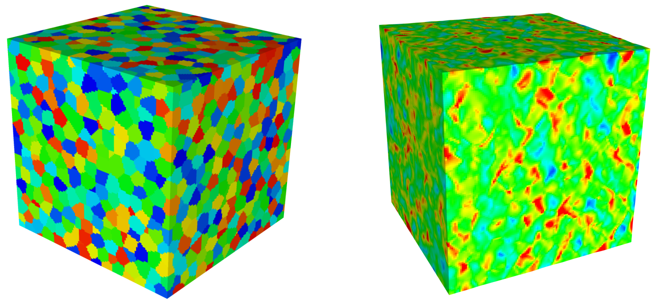

yield surface

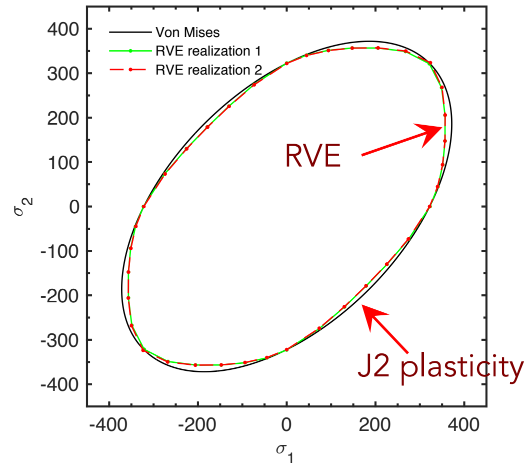

strain-rate dependence

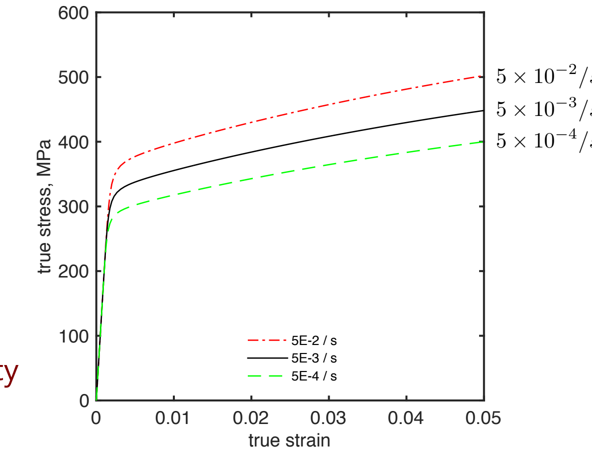

Comparison of stress fields

equi-axed,
no texture

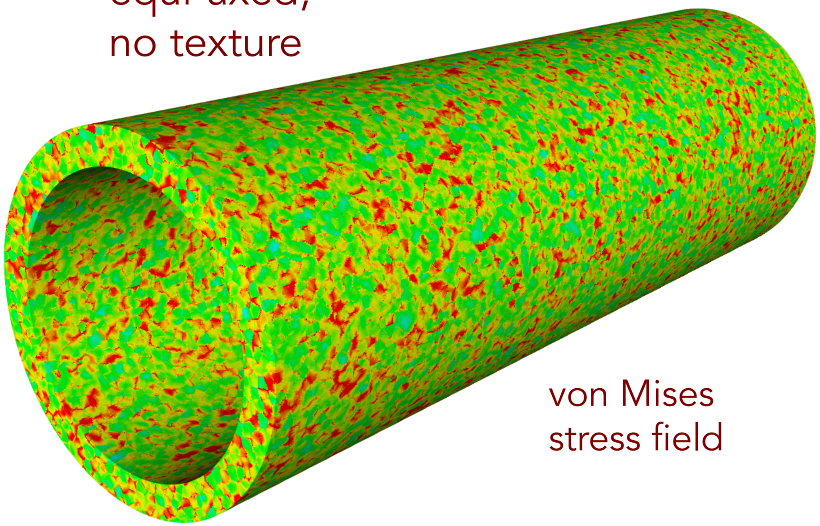

von Mises
stress field

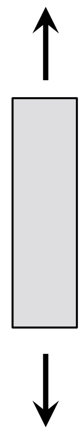

AM (KMC)
no texture

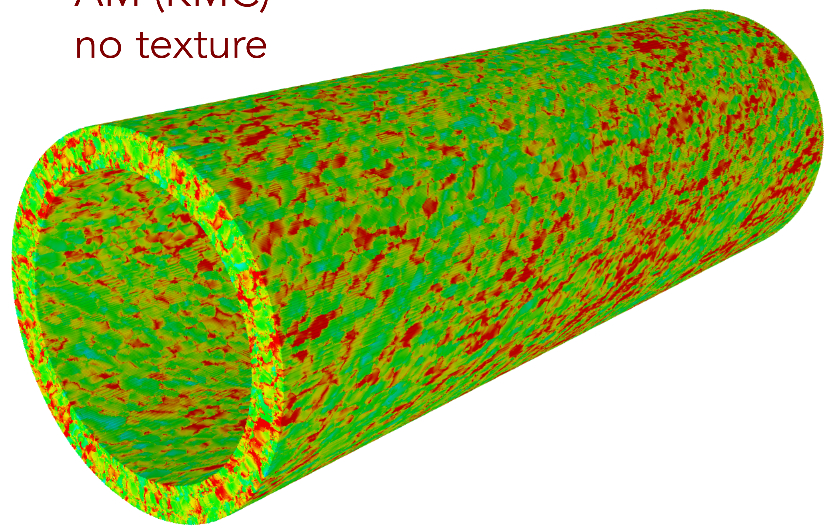

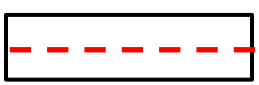

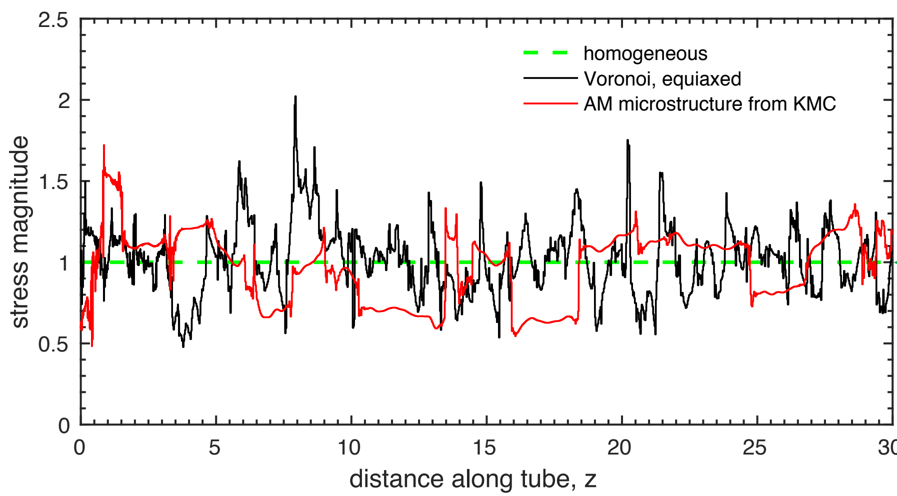

homogeneous
solution (constant)

Processing effects

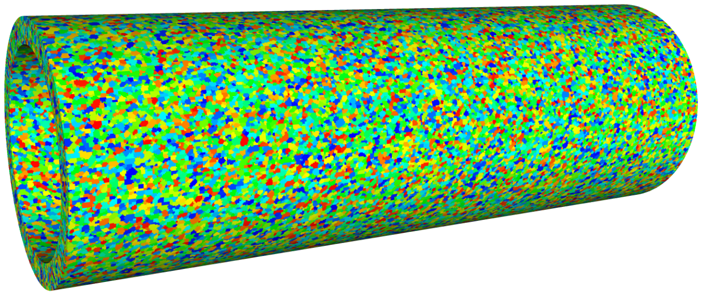

20 voxels/mcs

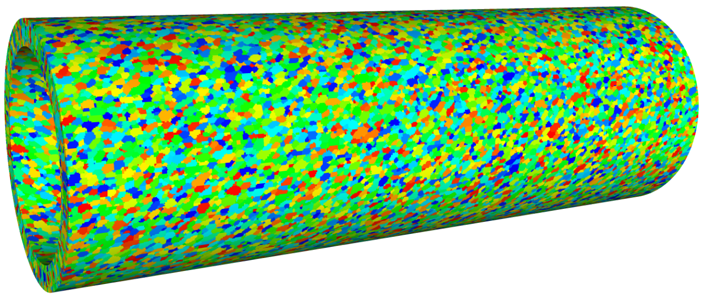

12.5 voxels/mcs

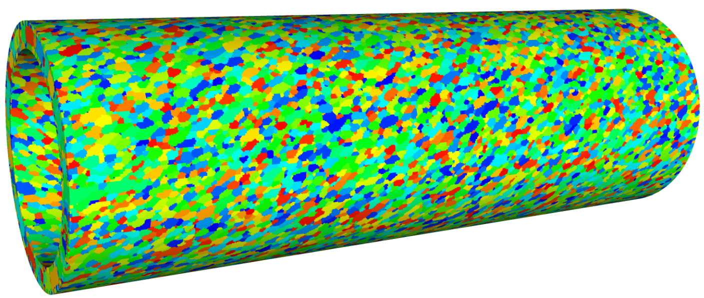

10 voxels/mcs

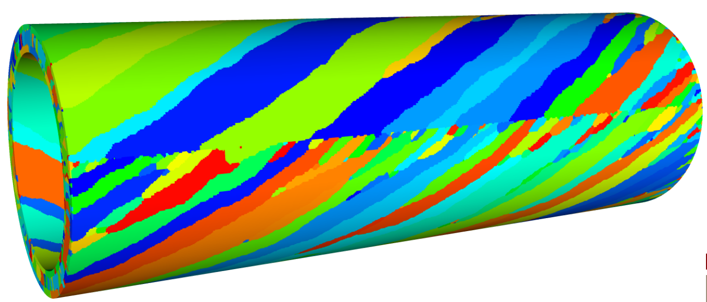

5 voxels/mcs

Laser speed = 20 voxels/mcs

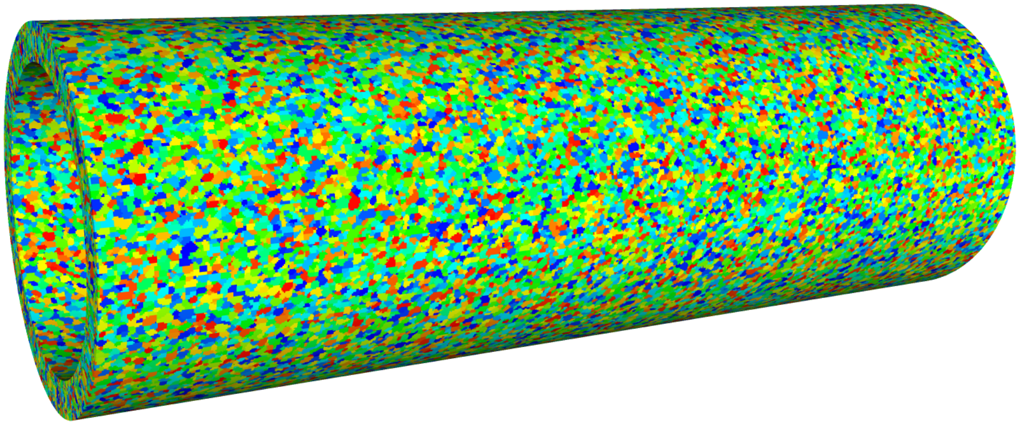

grain structure

Mises stress field in uniaxial tension

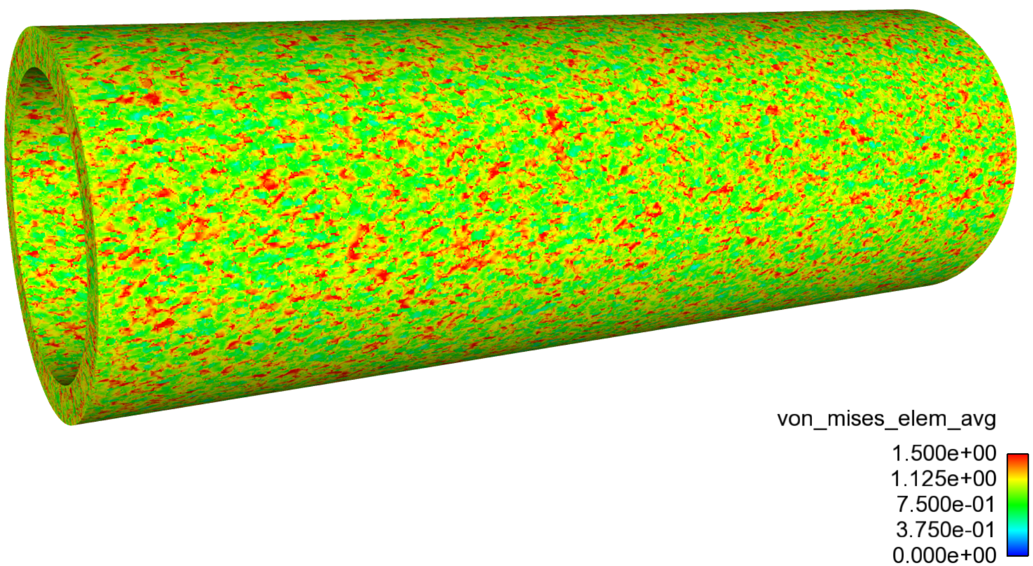

Laser speed = 12.5 voxels/mcs

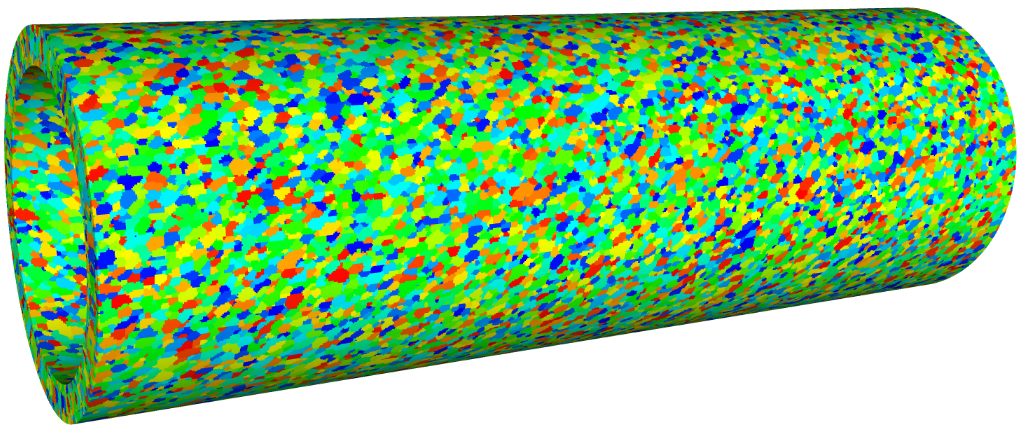

grain structure

Mises stress field in uniaxial tension

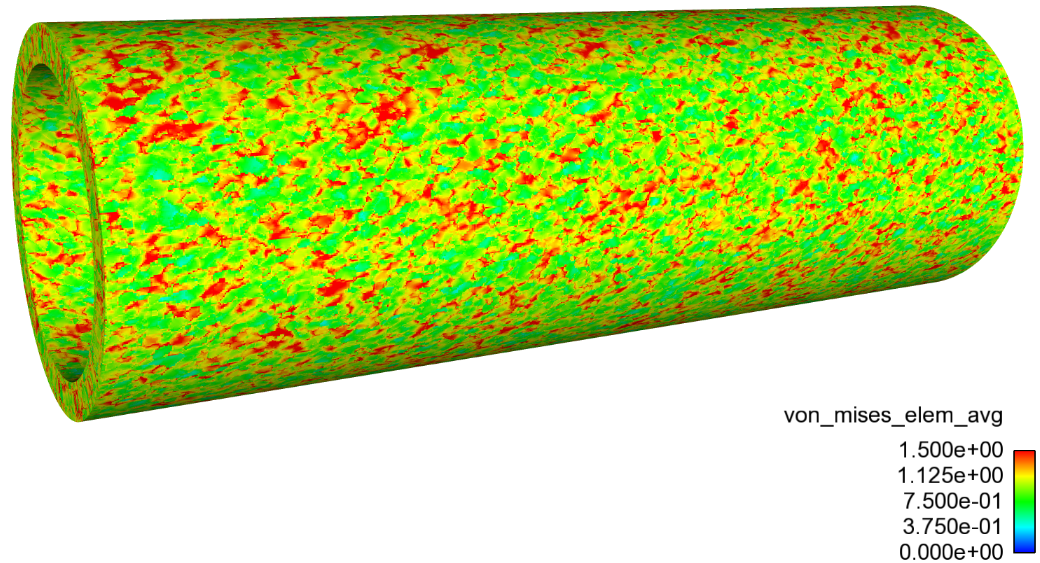

Laser speed = 10 voxels/mcs

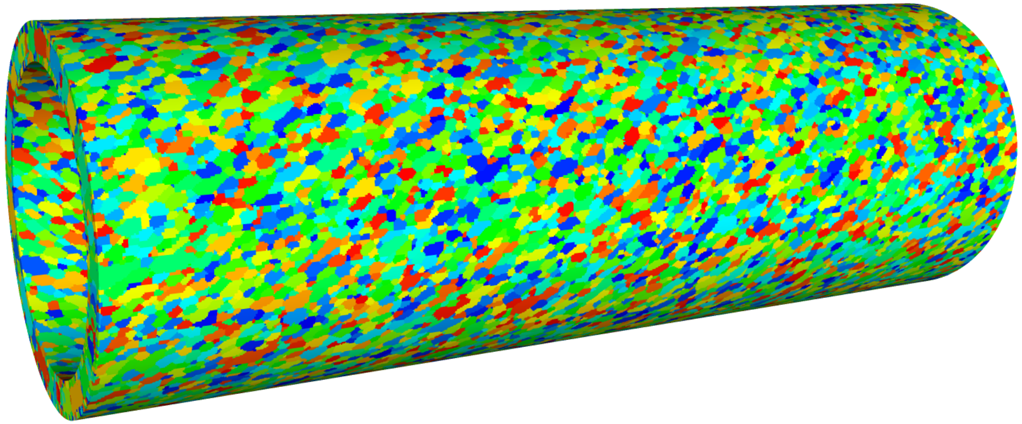

grain structure

Mises stress field in uniaxial tension

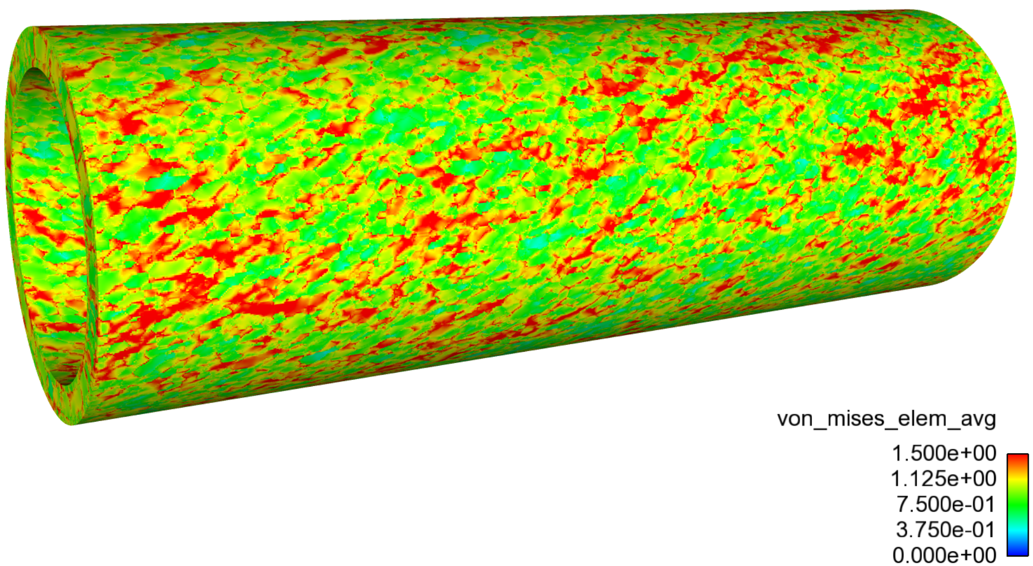

Laser speed = 5 voxels/mcs

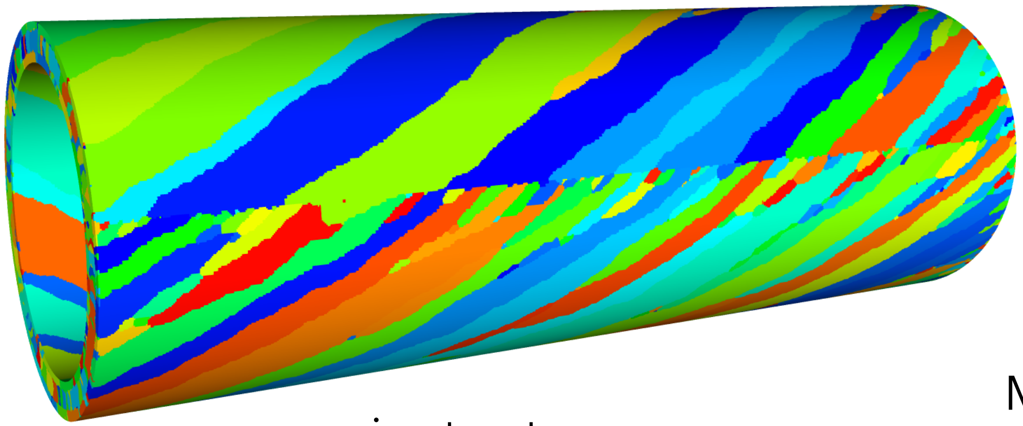

grain structure

Mises stress field in uniaxial tension

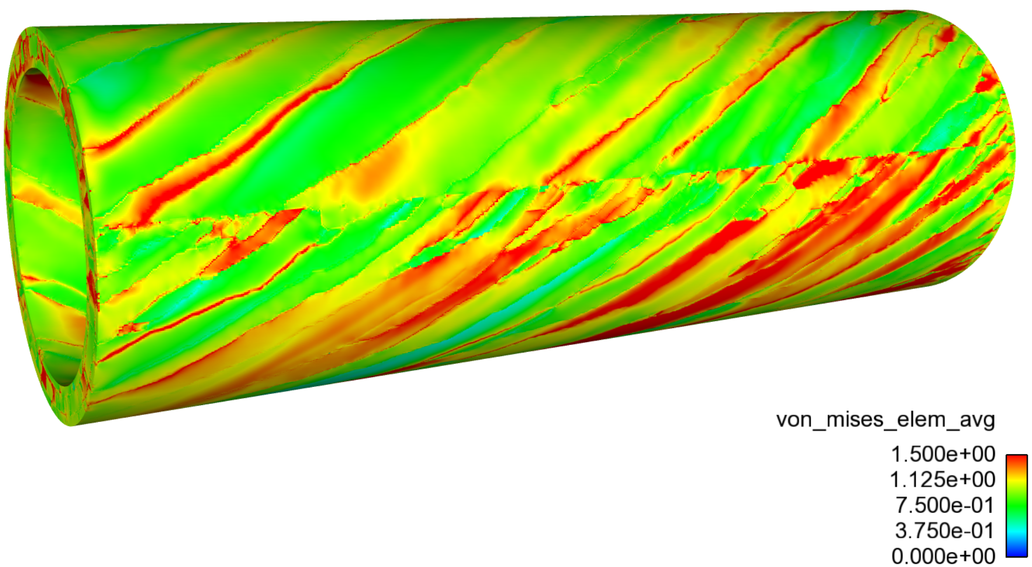

Comparison of local stress fields

5 voxels per mcs

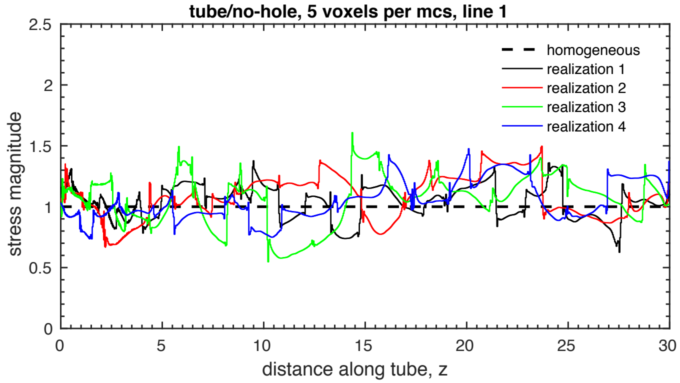

10 voxels per mcs

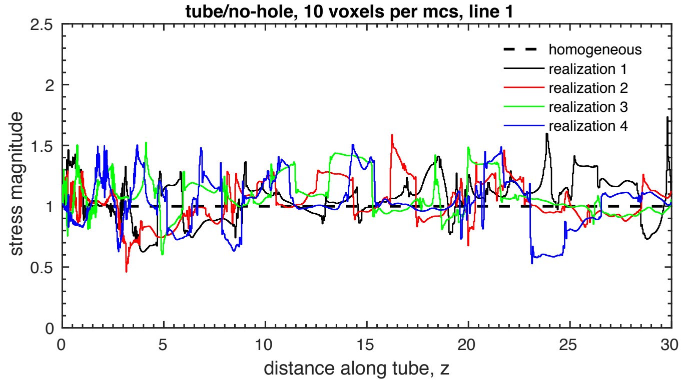

12.5 voxels per mcs

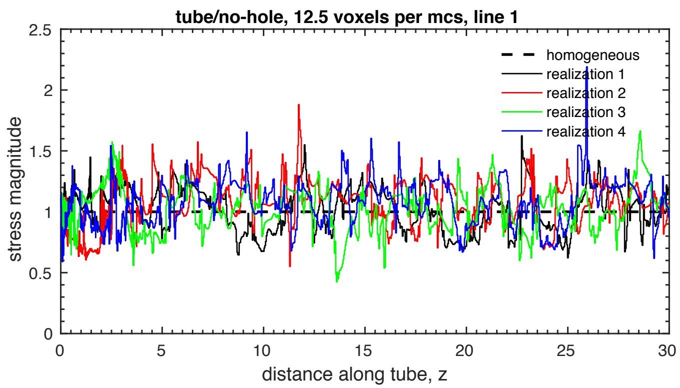

20 voxels per mcs

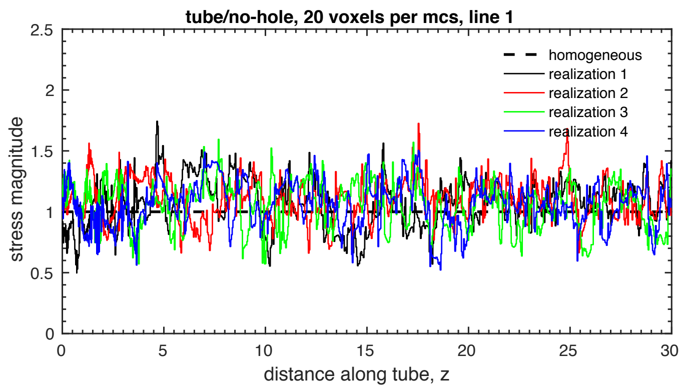

“Machining step”

- map to conformal finite-element mesh
- 30M elements

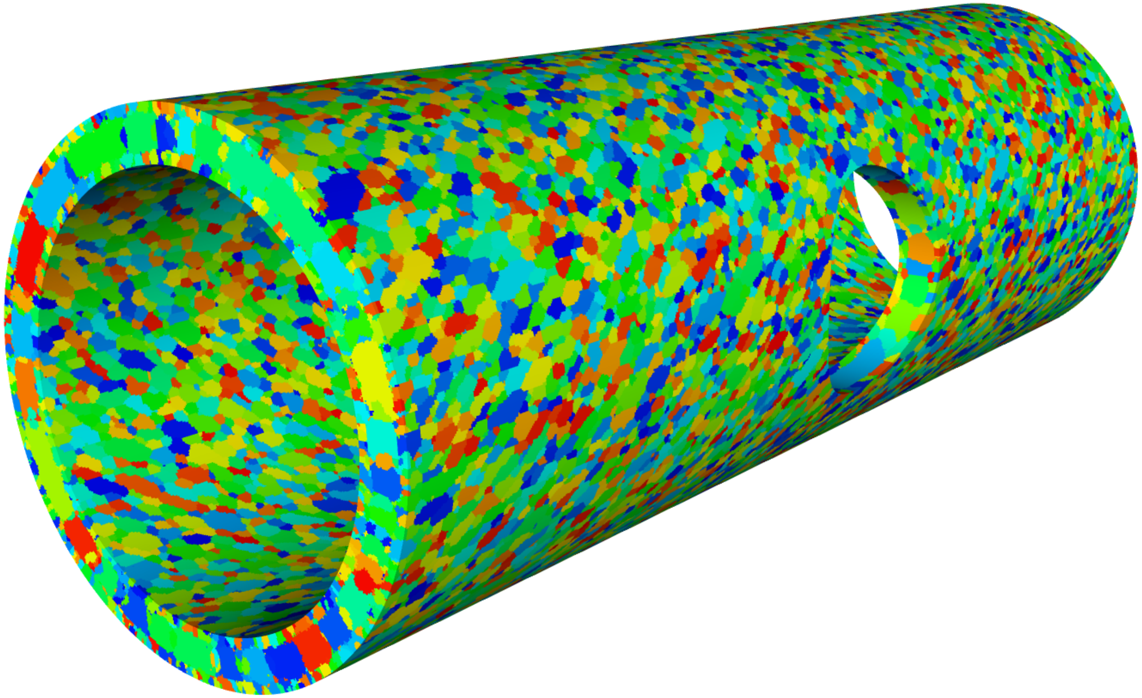

Homogeneous analysis results

- using homogenized material properties for wrought 304L
- isotropic (no texture)

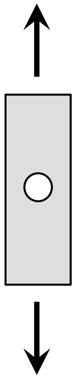

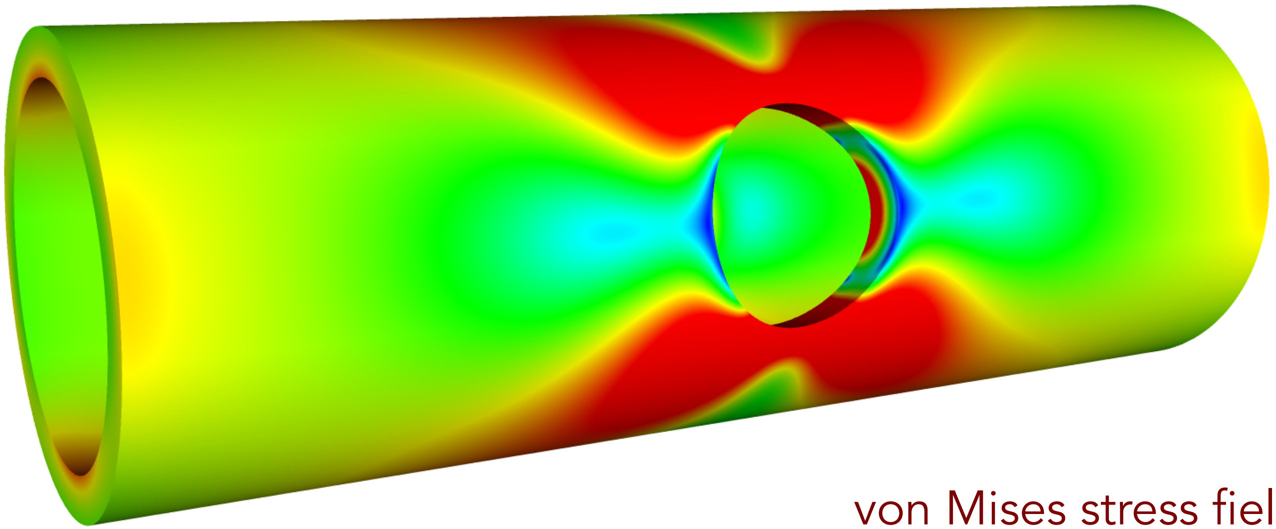

von Mises stress field

Laser speed = 20 voxels/mcs

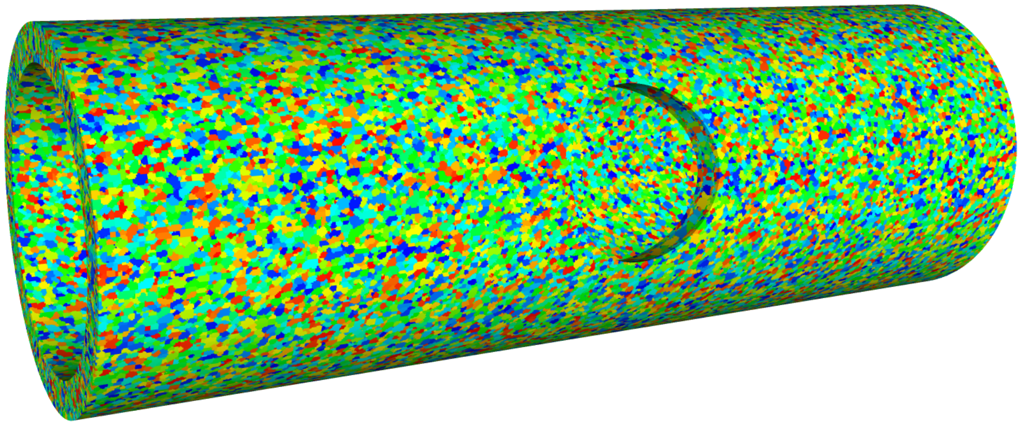

grain structure

Mises stress field in uniaxial tension

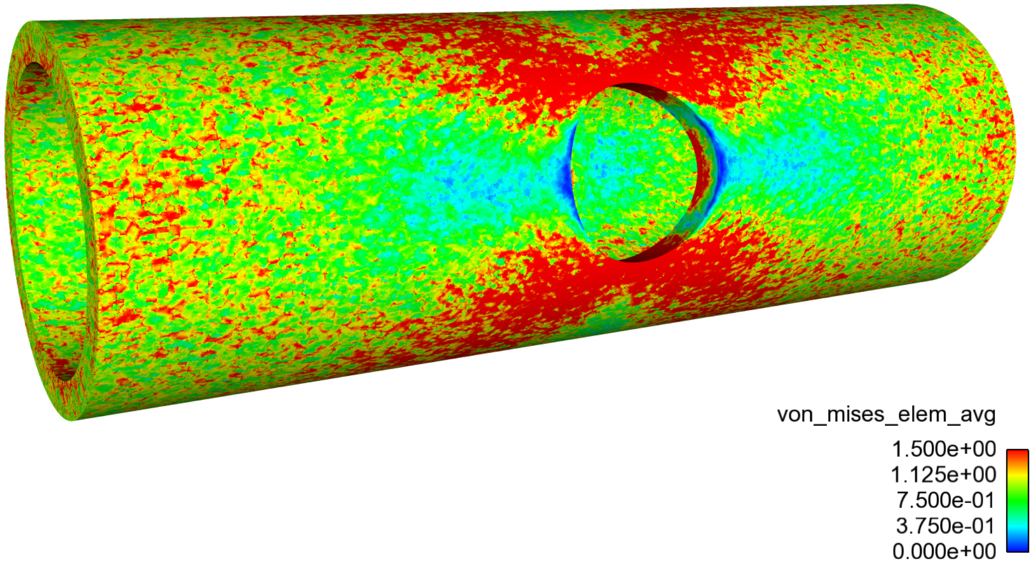

Laser speed = 12.5 voxels/mcs

Sandia National Laboratories

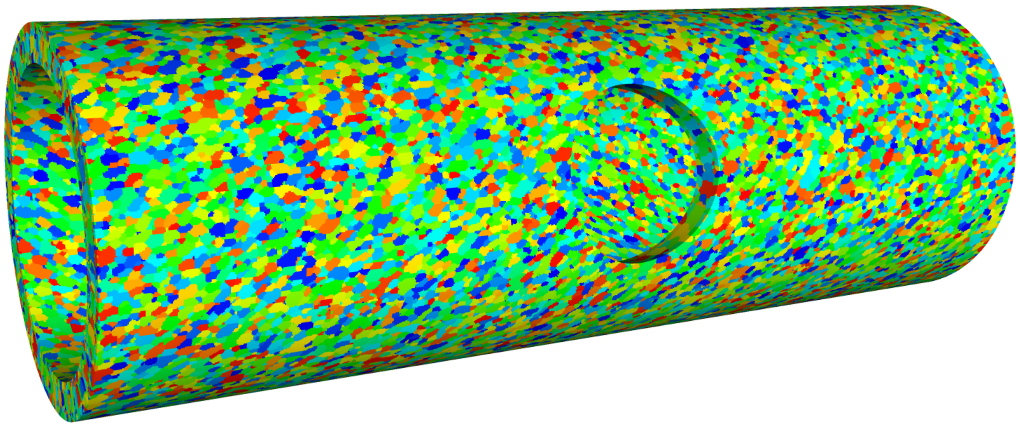

grain structure

Mises stress field in uniaxial tension

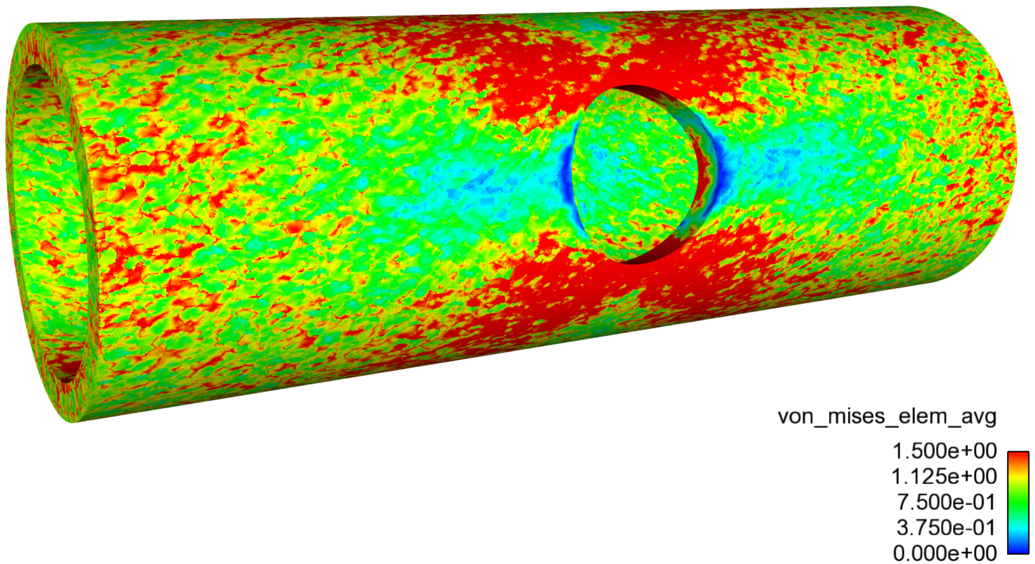

Laser speed = 10 voxels/mcs

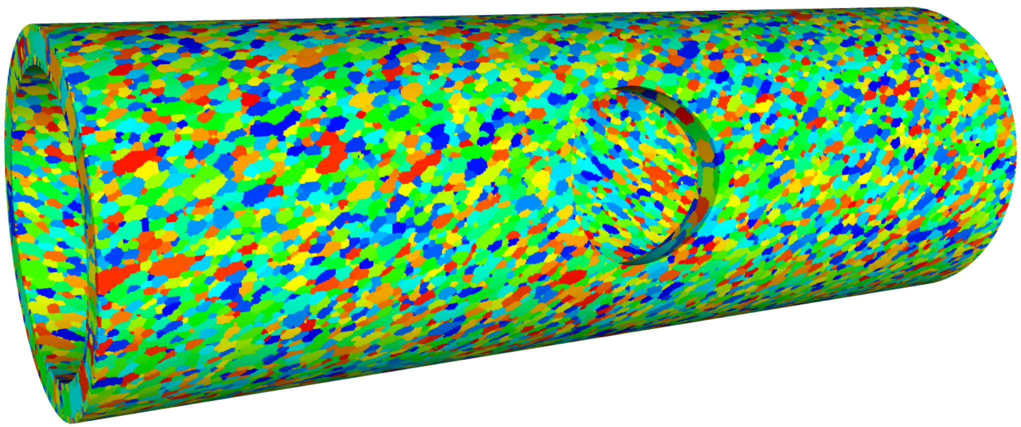

grain structure

Mises stress field in uniaxial tension

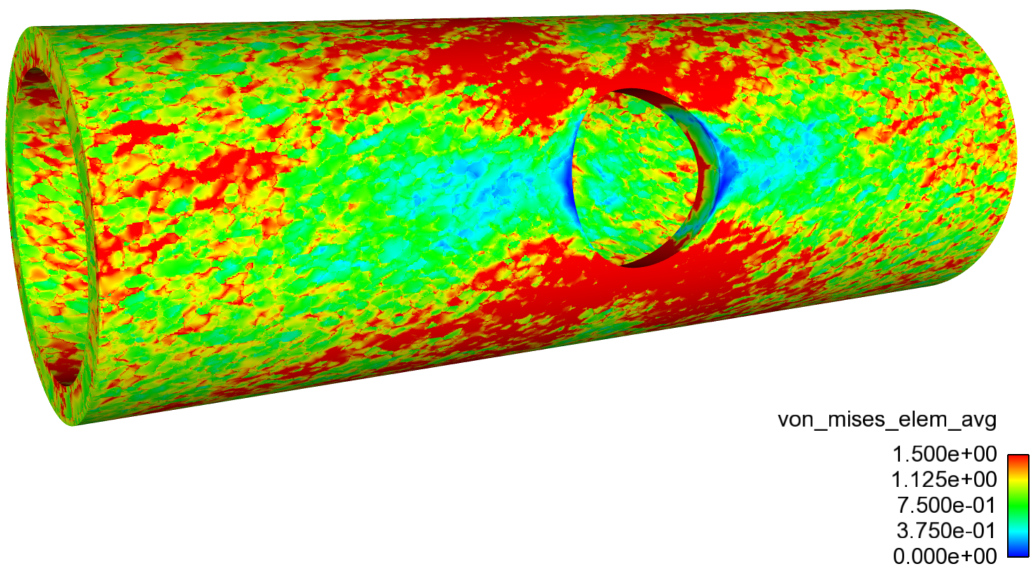

Laser speed = 5 voxels/mcs

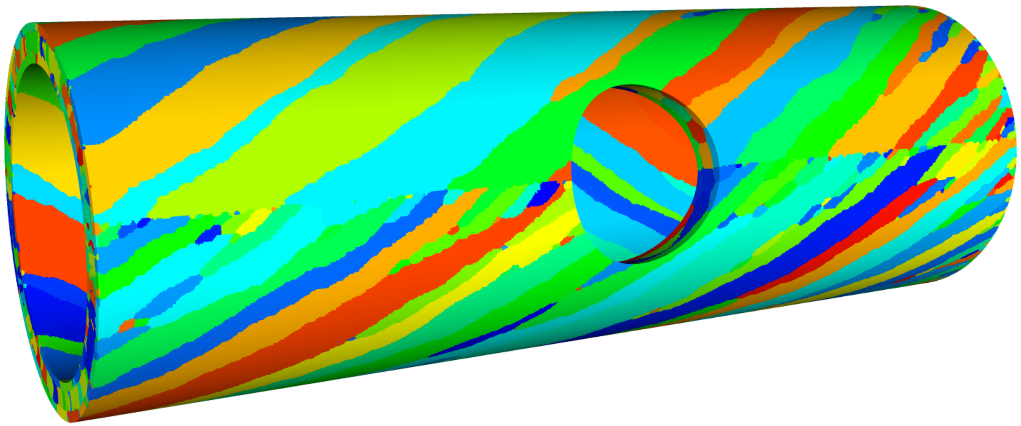

grain structure

Mises stress field in uniaxial tension

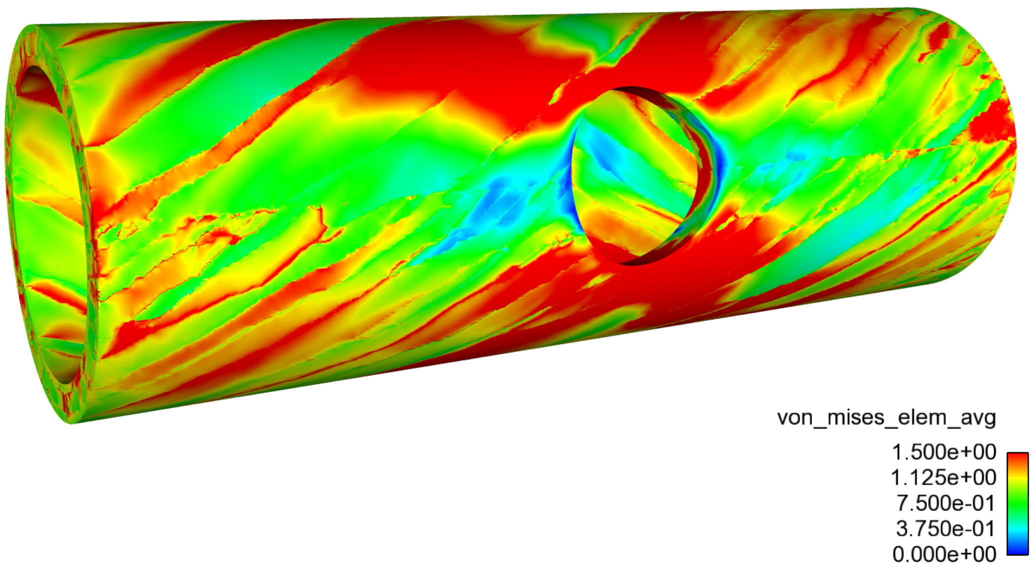

Comparison of local stress fields

line along length of tube (between holes)

5 voxels per mcs

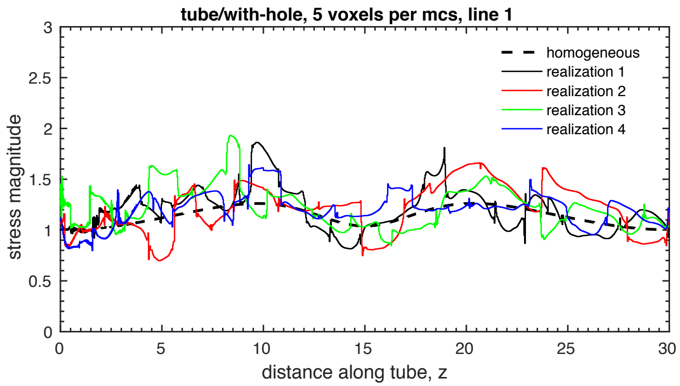

10 voxels per mcs

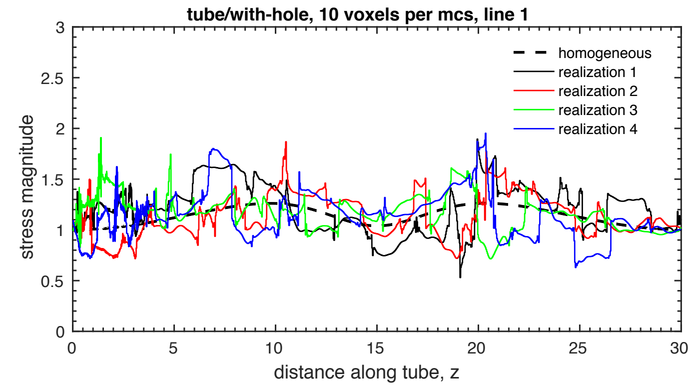

12.5 voxels per mcs

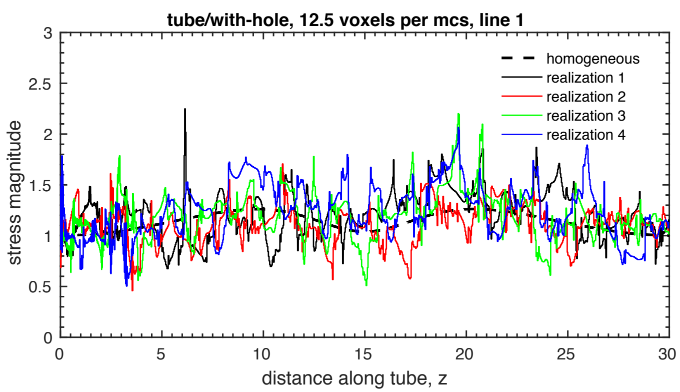

20 voxels per mcs

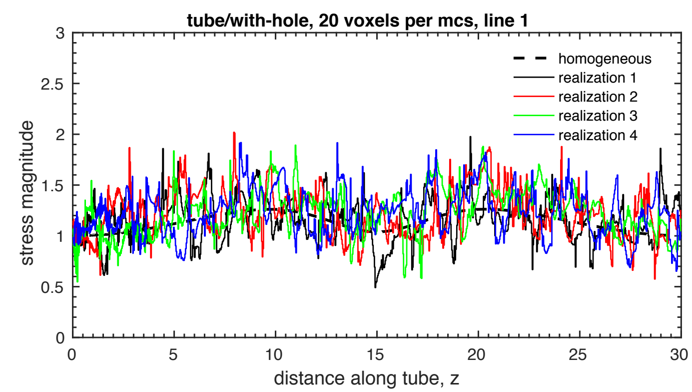

Comparison of local stress fields

(curve around hole)

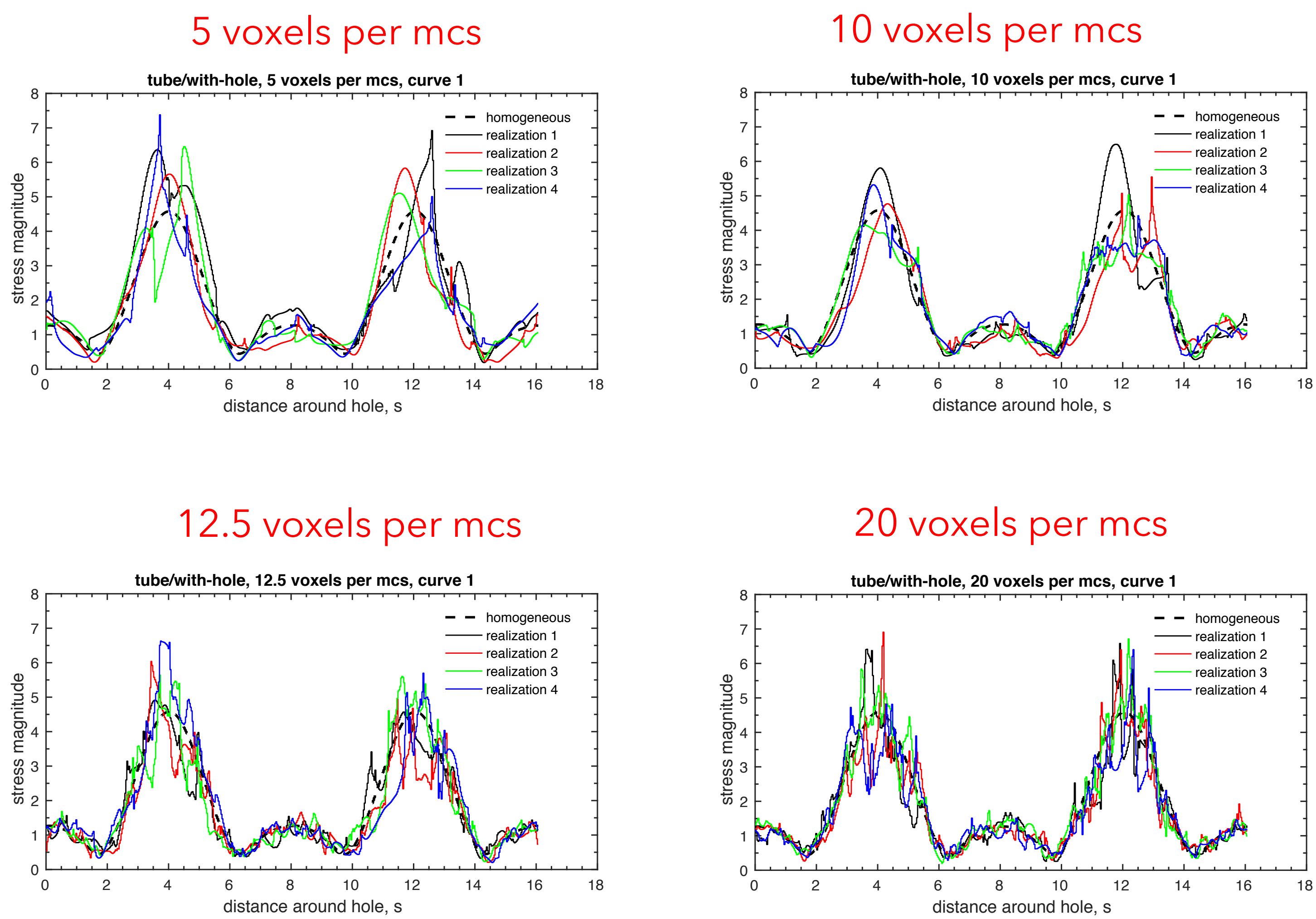

DNS modeling is impractical for engineering scale simulations (even with future exascale).

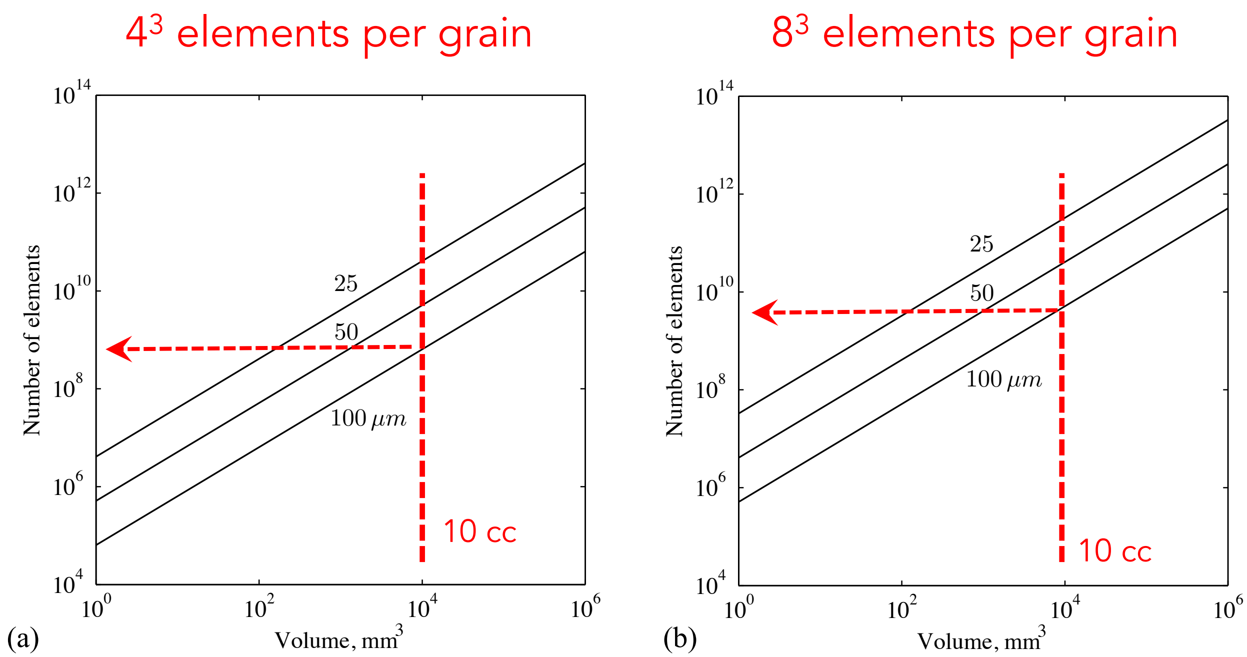

Homogenization-Localization Duality

Homogenize (filter fine scale)

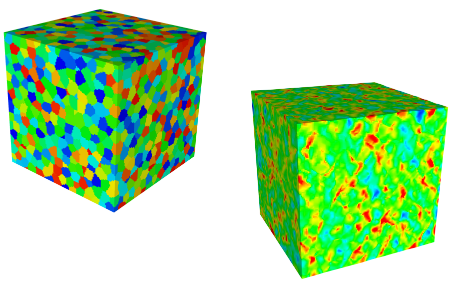

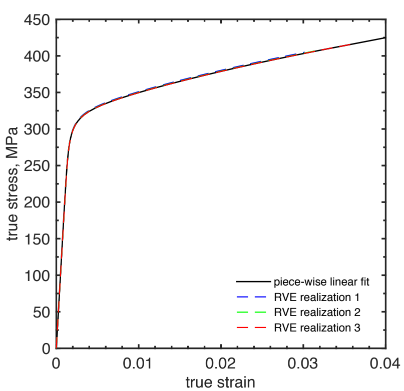

Macroscale simulation

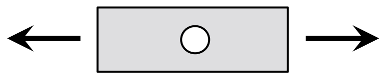

$$\frac{\partial \mathbf{P}}{\partial \mathbf{X}} : \mathbf{I} + \rho_o \mathbf{b} = \rho_o \ddot{\mathbf{u}} \quad \text{in} \quad \Omega$$

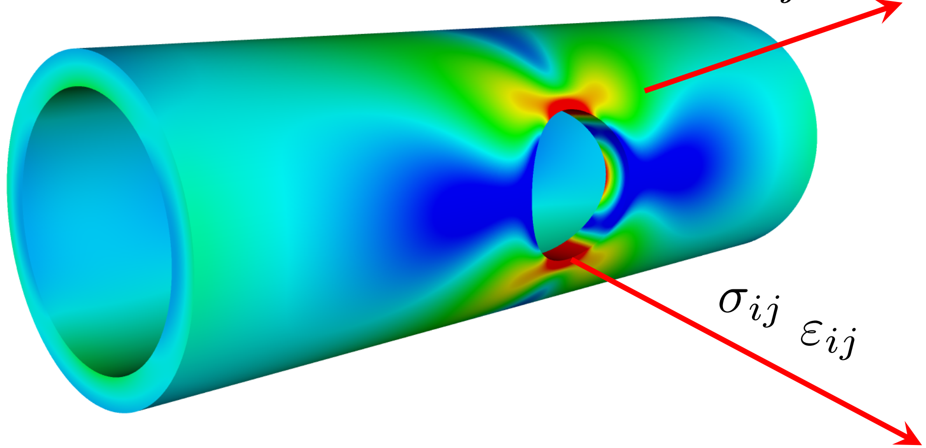

Localization (recover fine scale)

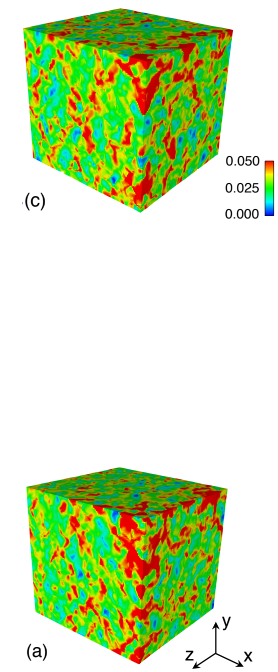

Assumptions:

- scale separation
- RVE well defined
- no surface effects

Error estimation: single scale

(Zohdi, Oden, Rodin, 1996, "Hierarchical modeling of heterogeneous bodies", CMAME)

$$||\mathbf{u} - \mathbf{u}^0||_E^2 \leq \int_\Omega (\boldsymbol{\varepsilon}^0 - \bar{\boldsymbol{\varepsilon}}) : (\bar{\boldsymbol{\sigma}} - \boldsymbol{\sigma}^0)\, d\Omega$$

- $\mathbf{u}$: displacement field using true material model
- $\mathbf{u}^0$: approximate displacement field from simplified or approximate material model
- $\bar{\boldsymbol{\varepsilon}}$: strain field resulting from approx. stress field but true material model
- $\bar{\boldsymbol{\sigma}}$: stress field resulting from approx. strain field but true material model

<u>Key point</u>: Can bound error using only known quantities from the approximate simulation. Don't need to run "true" model simulation.

Error estimation: multi-scale

Previous error estimate will perform poorly if applied here.

- similar to Voigt assumption in composites theory (uniform strain)
- need to use a modified error estimate in energy norm.

(Oden, Zohdi, 1997)

$$||\mathbf{w} - \mathbf{u}||_E^2 = 2[J(\mathbf{w}) - J(\mathbf{u}^0)] + ||\mathbf{u} - \mathbf{u}^0||_E^2$$

approximate displacement field

displacement field using true material model

potential energy functional

previous estimate

$$||\mathbf{u} - \mathbf{u}^0||_E^2 \leq \sum_{i=1}^{N} V_e \, \eta_i^2$$

How to get approximate microscale displacement field, w?
use a Dirichlet projection (submodeling)

Multi-scale error estimation and UQ

- Localization: Use macroscale solution to recover fine-scale solution.
- Key idea: apply displacements from macroscale solution to "cut" surfaces of each subdomain, and re-solve boundary value problem to get updated solution on interior.
- Also called "Dirichlet projection", or "submodeling."
- Two types: non-overlapping (Type 1) and overlapping (Type 2)

First, partition structure into non-overlapping subdomains.

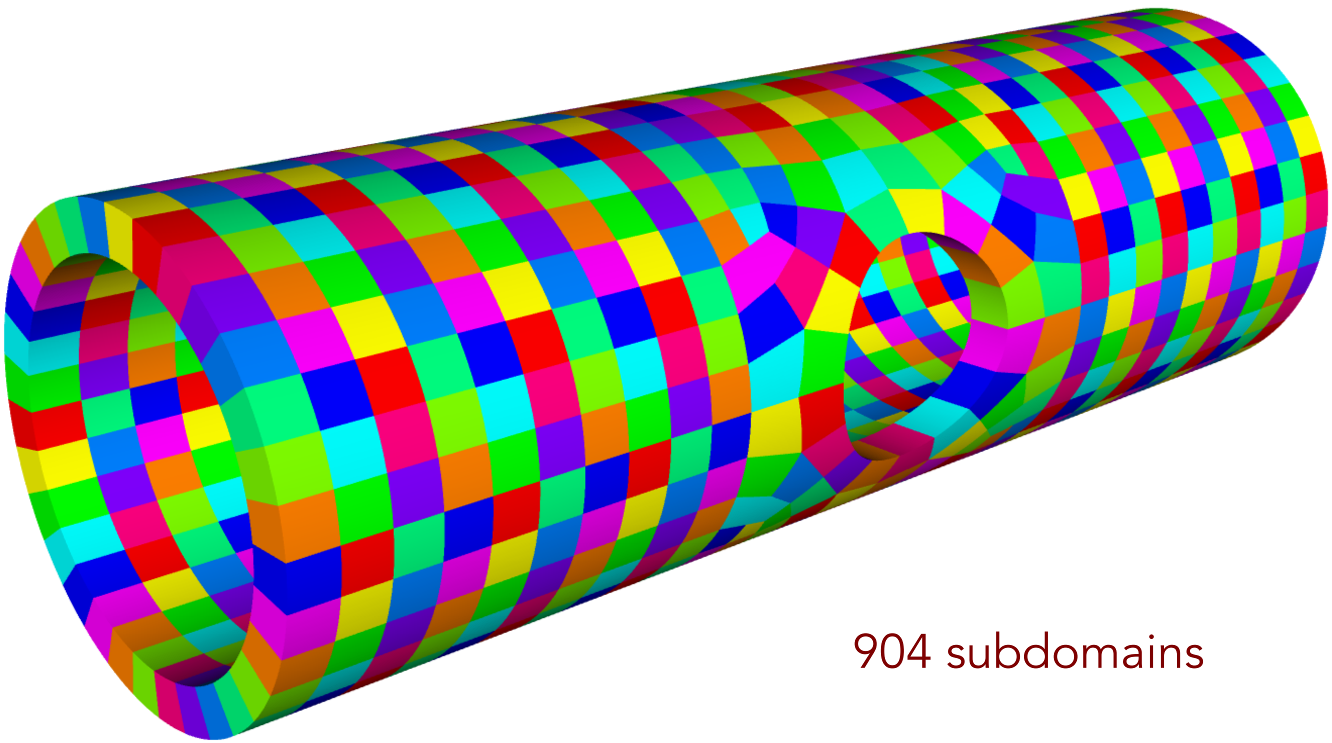

904 subdomains

Type 1 localization

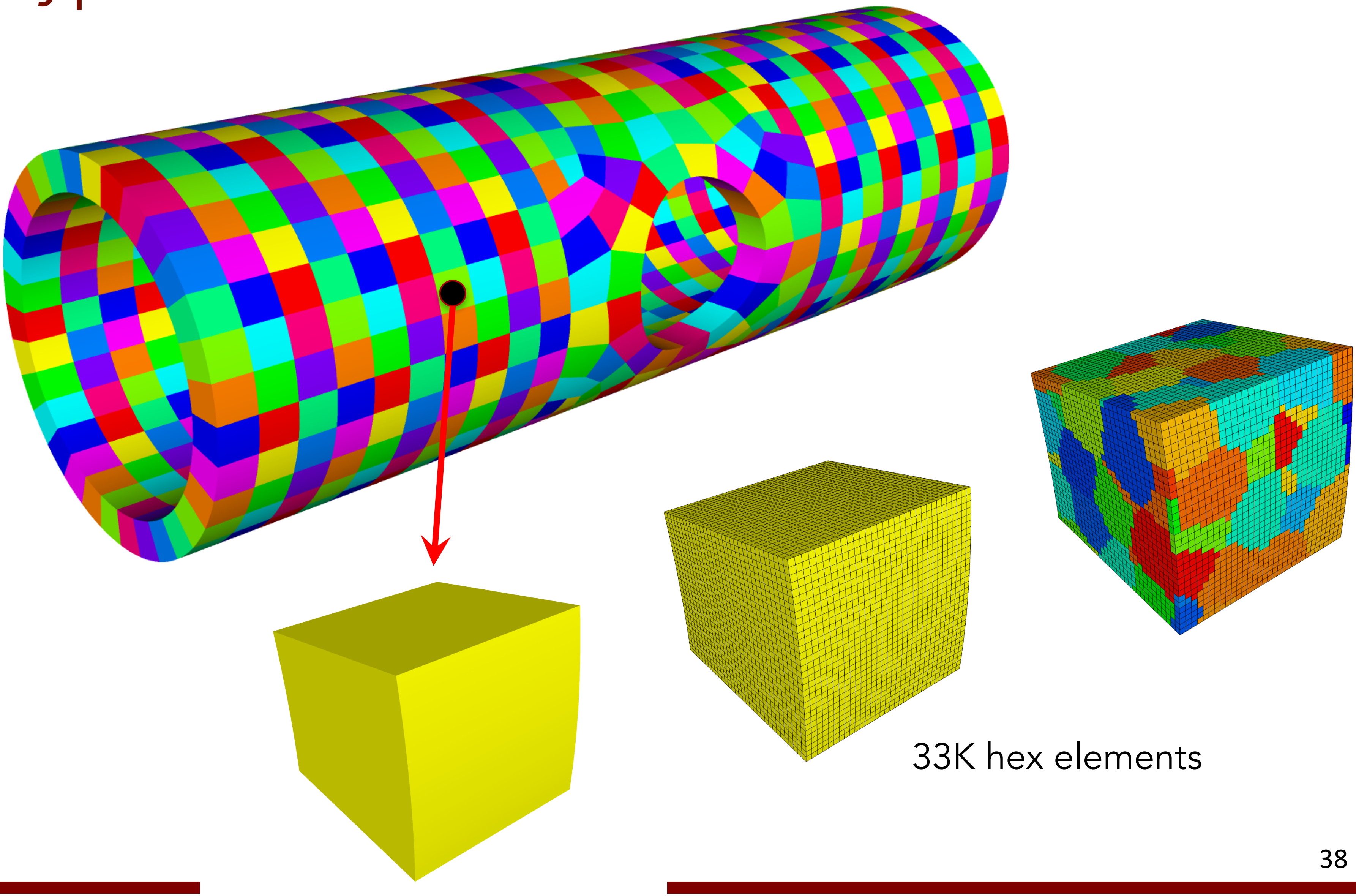

33K hex elements

Type 1 localization

Sandia National Laboratories

submodel

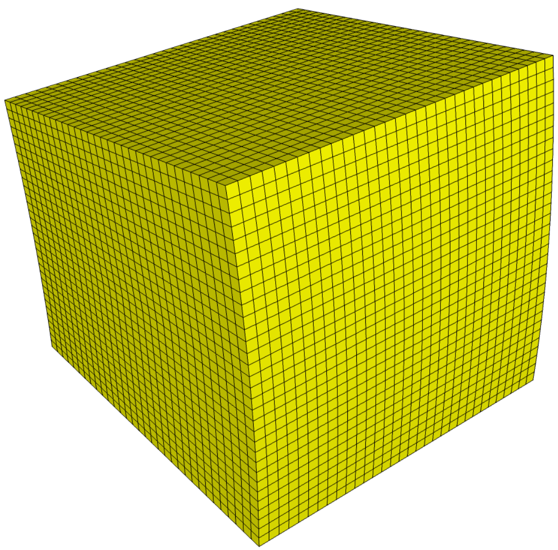

33K hex elements

displacement b.c.s

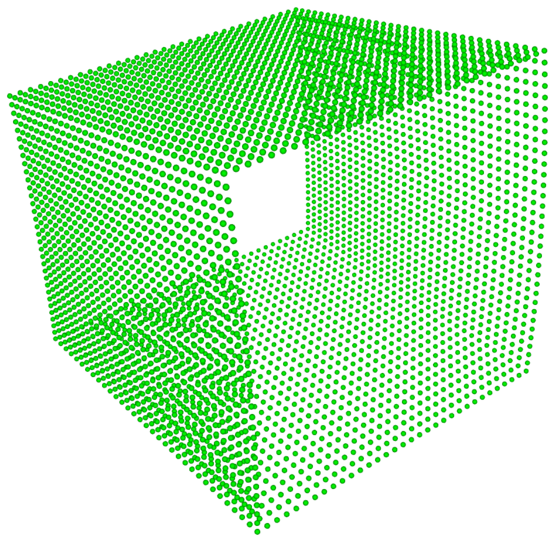

traction b.c.s

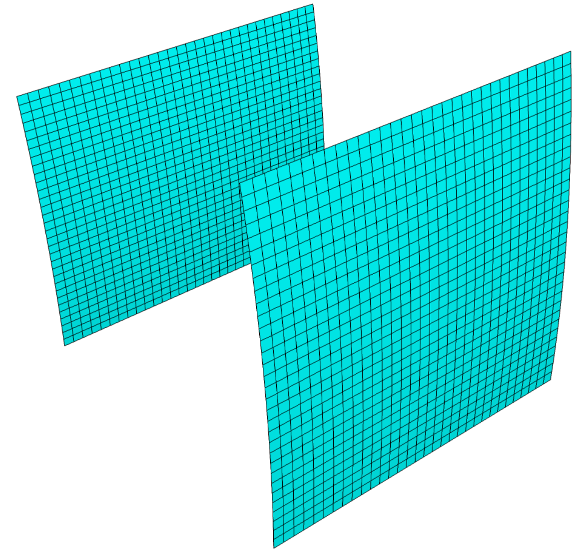

local stress field

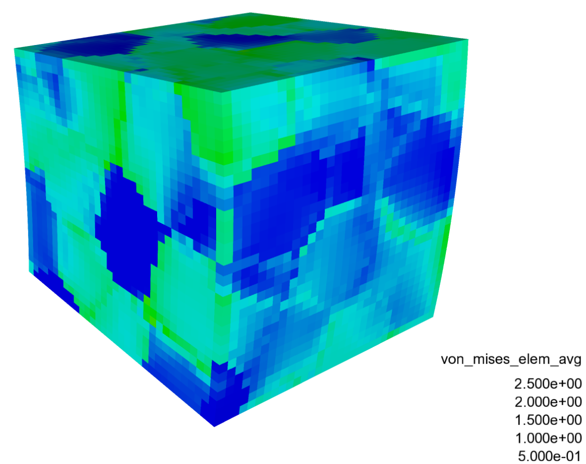

Type 2 localization (overlapping)

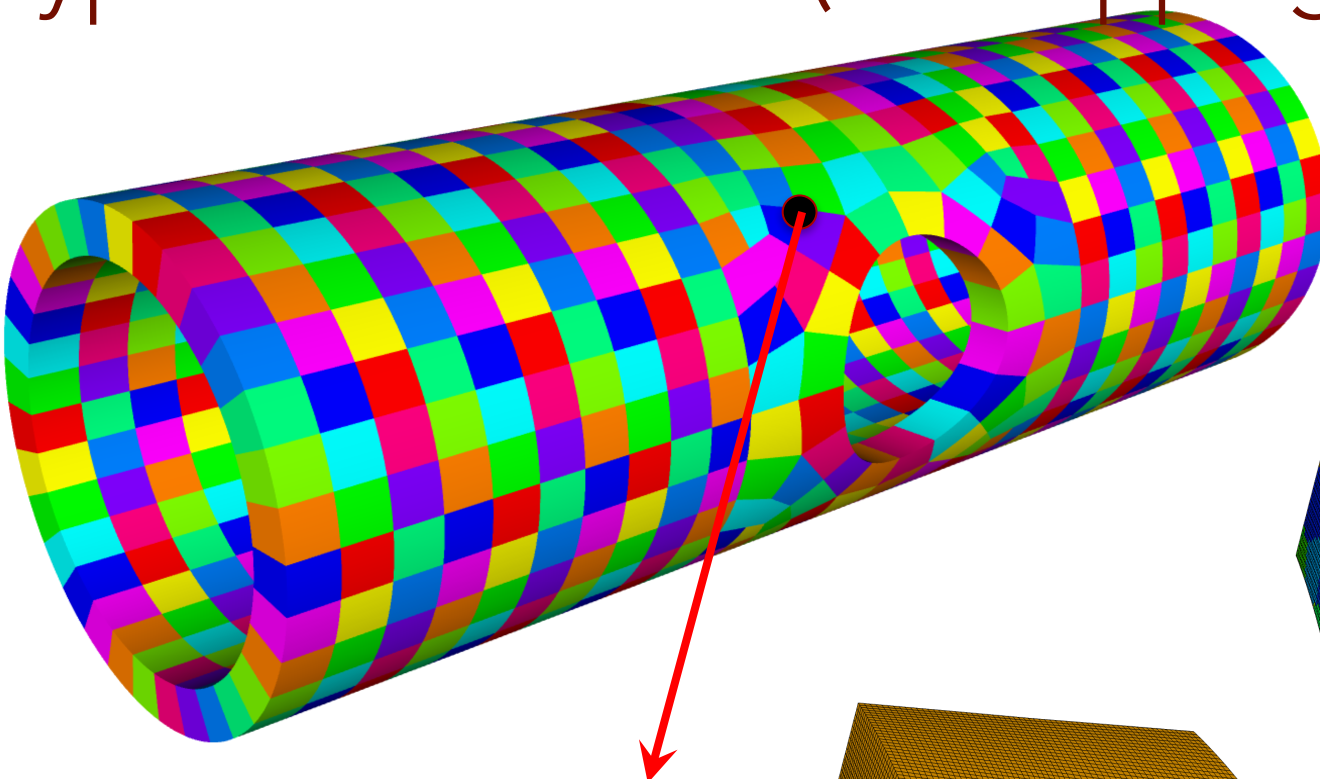

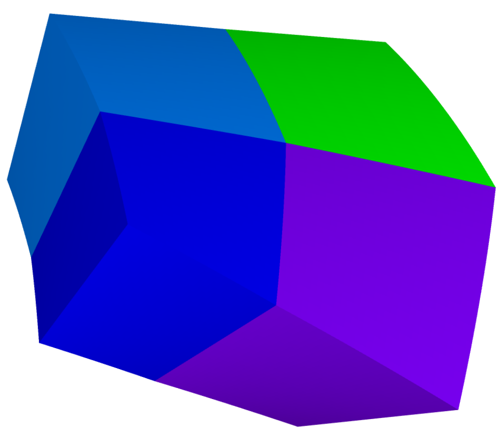

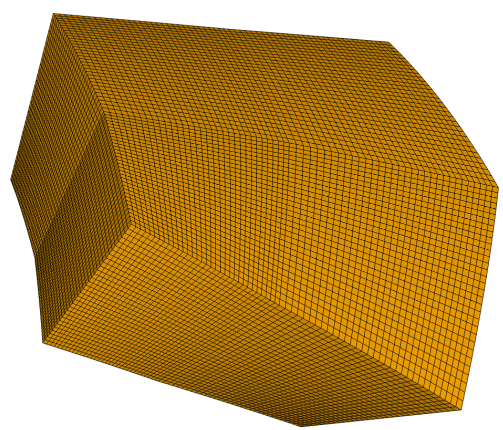

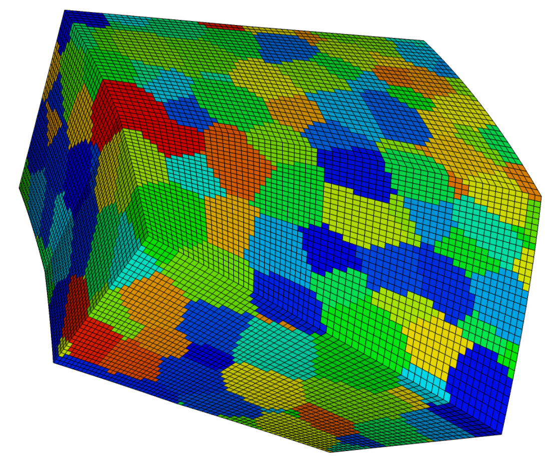

130K hex elements

Type 2 localization

submodel

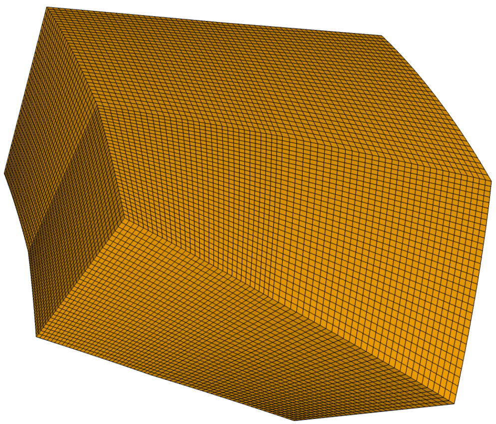

displacement b.c.s

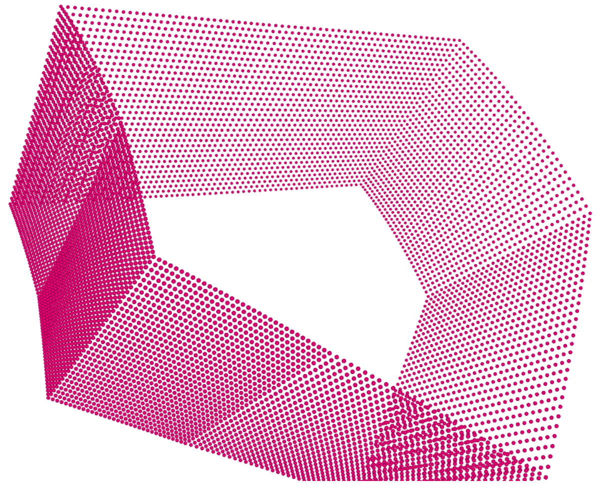

traction b.c.s

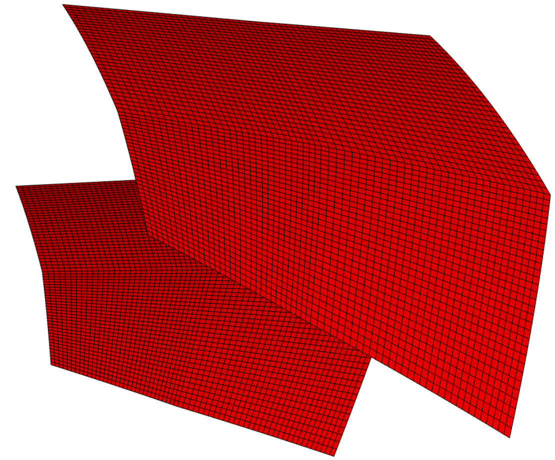

local stress field

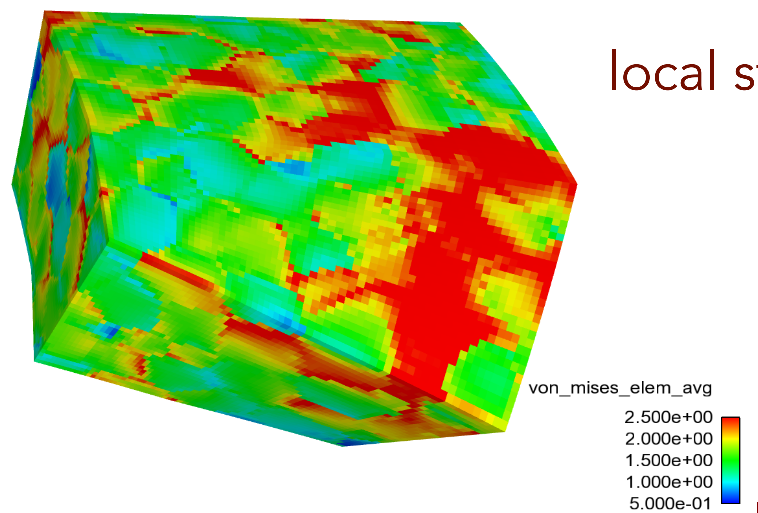

Localization results (equiaxed)

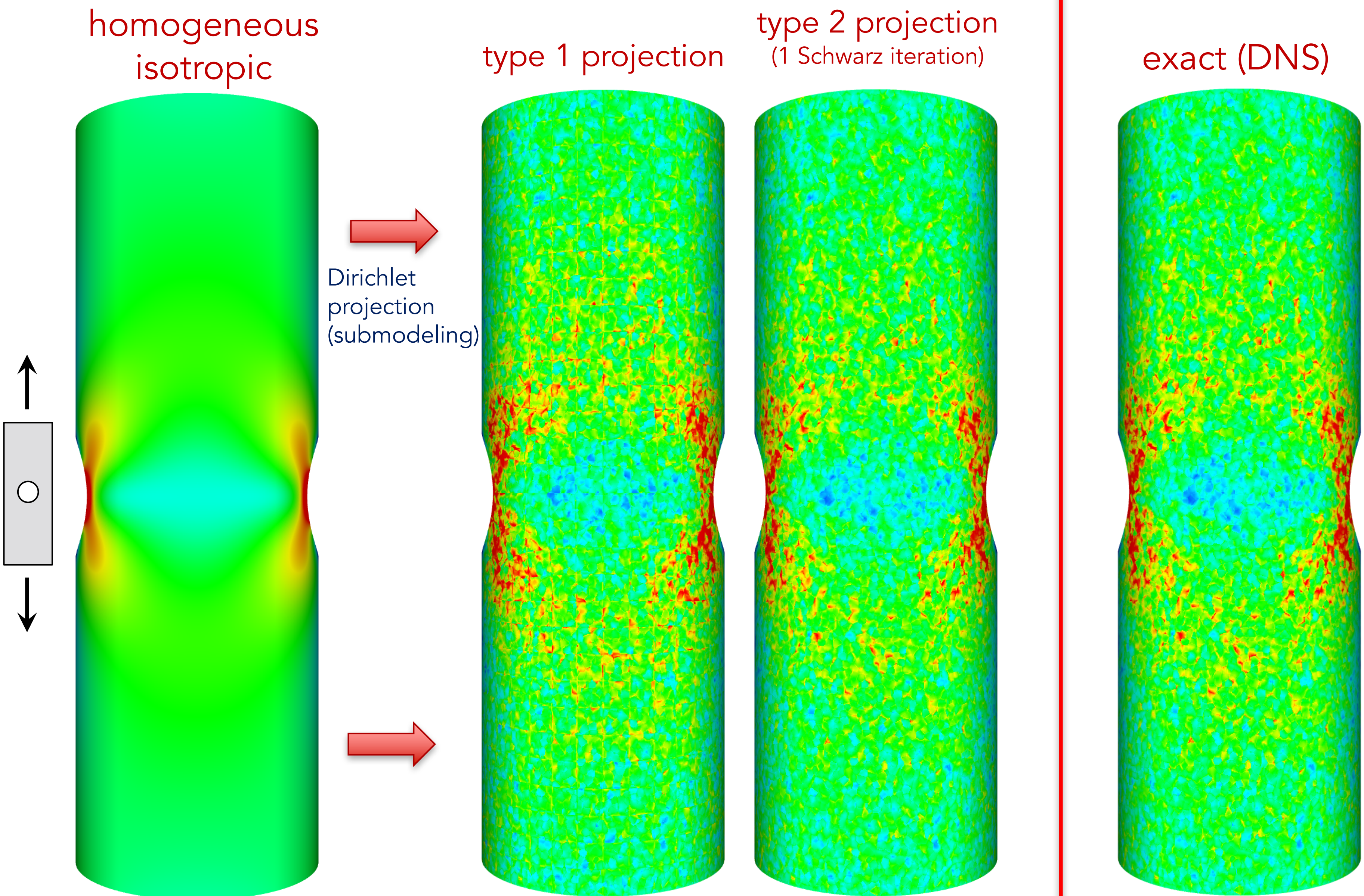

Localization results (AM)

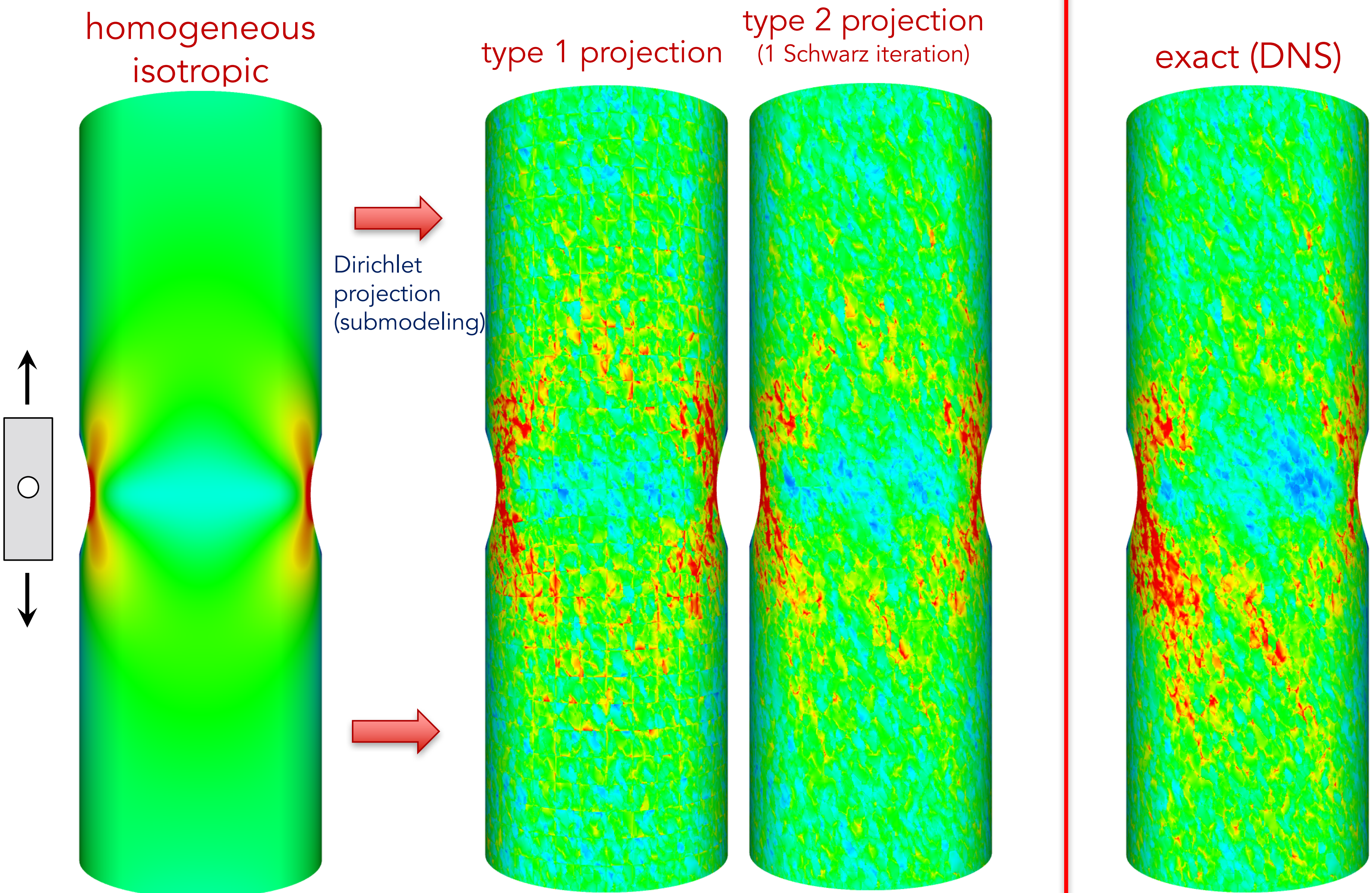

Adaptive macroscale properties

How to update macroscale properties (apparent) to minimize error?

- Use current approximate stress, strain fields

minimize $e = ||\langle \sigma_{ij} \rangle - \mathbb{C}^0 \langle \varepsilon_{ij} \rangle||^2$ by choosing C^0

let C^0 be isotropic $\mathbb{C}^0 = \mathbb{C}^{\text{iso}} = a\,\mathbb{J} + b\,\mathbb{K} = 3K\,\mathbb{J} + 2\mu\,\mathbb{K}$

necessary conditions $\frac{\partial e}{\partial a} = 0 \quad \text{and} \quad \frac{\partial e}{\partial b} = 0$

result $3K = \frac{\langle \sigma_{kk} \rangle}{\langle \varepsilon_{kk} \rangle} \qquad 2\mu = \frac{\text{dev}\langle \sigma_{ij} \rangle : \text{dev}\langle \sigma_{ij} \rangle}{\text{dev}\langle \varepsilon_{ij} \rangle : \text{dev}\langle \varepsilon_{ij} \rangle}$

Summary

1. Investigating use of *a posteriori* error estimation techniques for quantifying homogenization errors and other model-form errors.
2. both single scale and multi-scale
3. application to AM and laser-welds

Future work

1. verify estimators are working, adaptivity of simple model
2. incorporation of texture in AM simulations
3. error in quantities of interest (goal oriented)
4. nonlinear (plastic) regime
5. multigrid concepts (multiple levels)

backup

Process – (micro) structure – performance (PSP) linkages

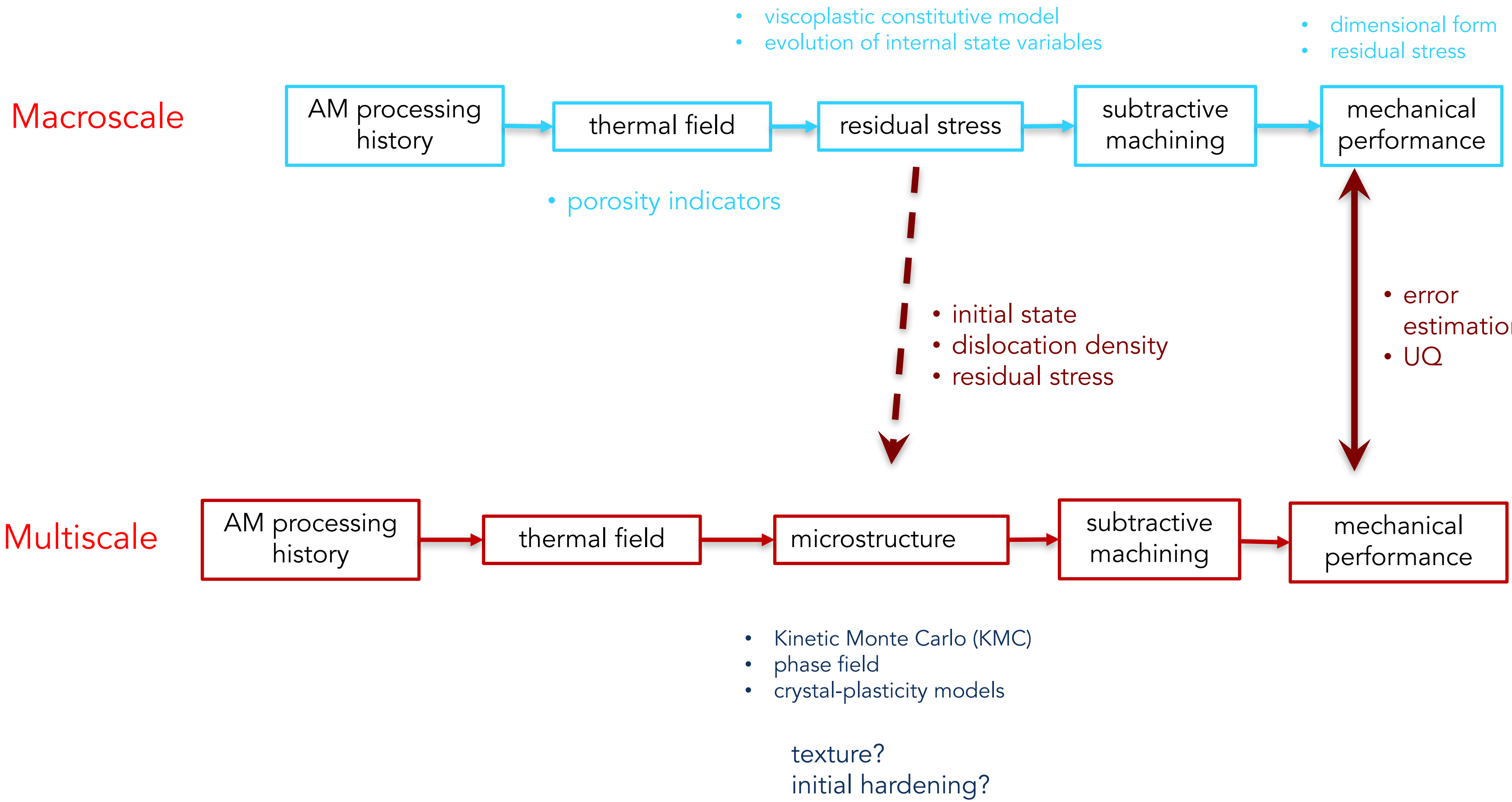

Types of errors (epistemic uncertainty)

- model-form error
- homogenization error
    - lack of scale separation
    - surface effects
    - lack of a representative volume element

Types of aleatory uncertainty

- microstructure (material variability)
- geometric
- loading

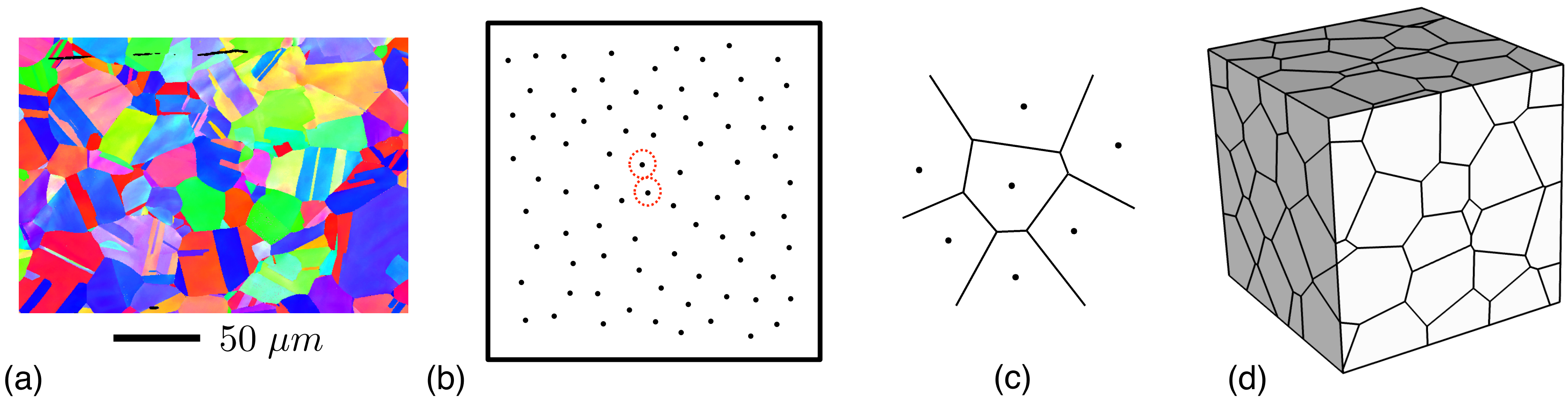
50 μm
(a)
(b)
(c)
(d)

Homogenization

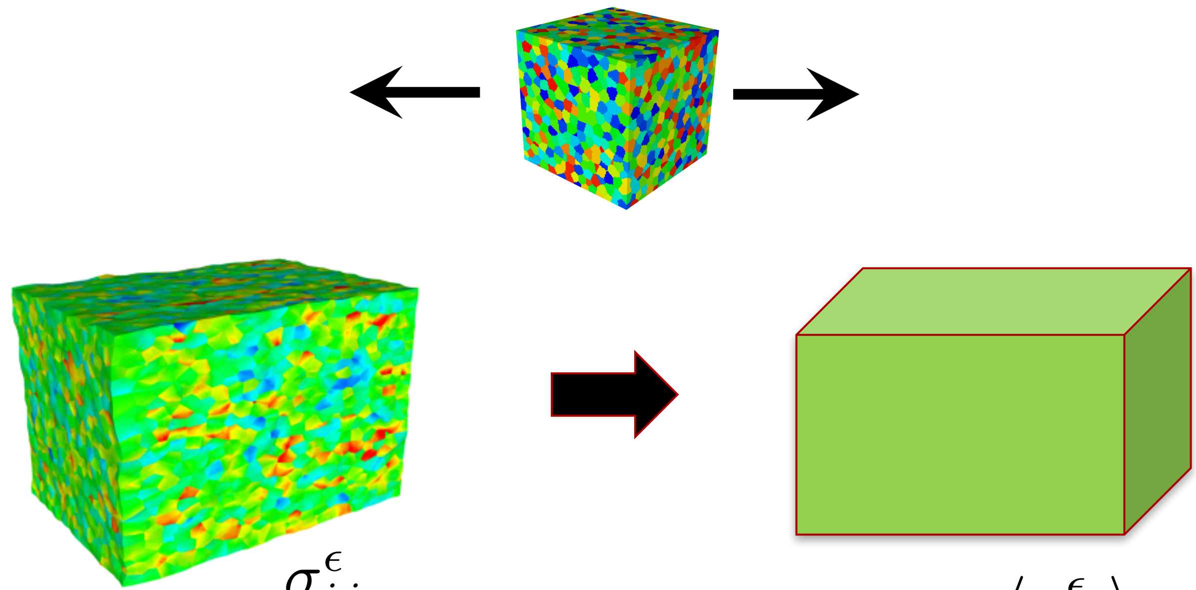

σ_{ij}^{ϵ}

fine-scale fluctuations

$\sigma_{ij} = \langle \sigma_{ij}^{\epsilon} \rangle$

replaced with mean behavior

This equivalence is also satisfied energetically: $\sigma_{ij}\varepsilon_{ij} = \langle \sigma_{ij}^{\epsilon} \rangle \langle \varepsilon_{ij}^{\epsilon} \rangle$

Constitutive models map average strain to average stress:

$$\varepsilon_{ij} = \langle \varepsilon_{ij}^{\epsilon} \rangle \longrightarrow \sigma_{ij} = \langle \sigma_{ij}^{\epsilon} \rangle$$

Kinetic Monte Carlo method for microstructure generation (Rodgers, et. al, JOM, 2016)

- The Monte Carlo Potts model evolves spins (or grain identifiers) on a discrete lattice to simulate microstructural evolution.
- Since the driving force for curvature-driven grain growth is the reduction in grain boundary energy, only grain boundary energy is considered and is given by the sum of the bond energies between neighboring lattice sites of unlike spins

system energy

$$E = \frac{1}{2}\sum_{i=1}^{N}\sum_{j=1}^{L}(1 - \delta(q_i, q_j))$$

N is total number of latttice sites
q_i and q_j are spins at lattice sites *i* and *j*
L is number of neighbors of each lattice site.

probability of accepting system change of state

$$P = \begin{cases} M \exp\left(\frac{-\Delta E}{k_B T_s}\right) & \text{if } \Delta E > 0 \\ M & \text{if } \Delta E \leq 0 \end{cases}$$

M is grain mobility (function of temperature)

- performed at a length scale that is much larger than required to resolve the formation and growth of dendrites
- this approach enables studying large numbers of grains and their evolution

Kinetic Monte Carlo method for microstructure generation

(Rodgers, et. al, JOM, 2016)

A 3D steady-state temperature profile with a given gradient G is rastered with a velocity V.

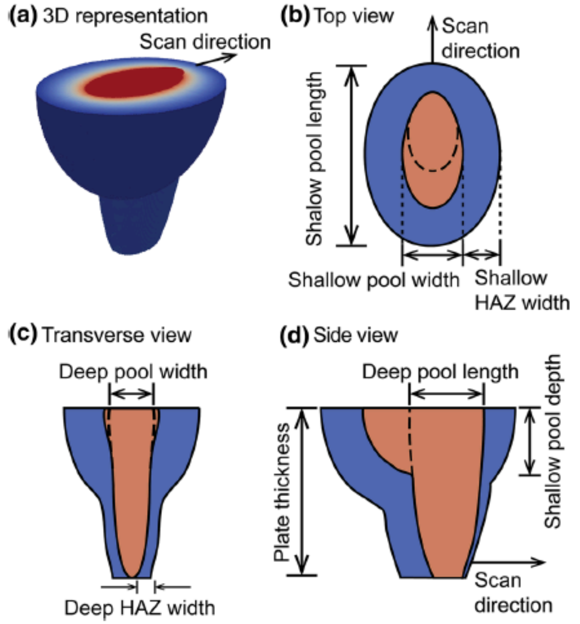

Fig. 1. (a) The 3D keyhole melt pool and temperature gradient used in the simulations. (b–d) Schematic cross sections of the melt pool and temperature field along orthogonal planes. In the schematics, the molten zone is shown in orange, while the surrounding HAZ is blue.

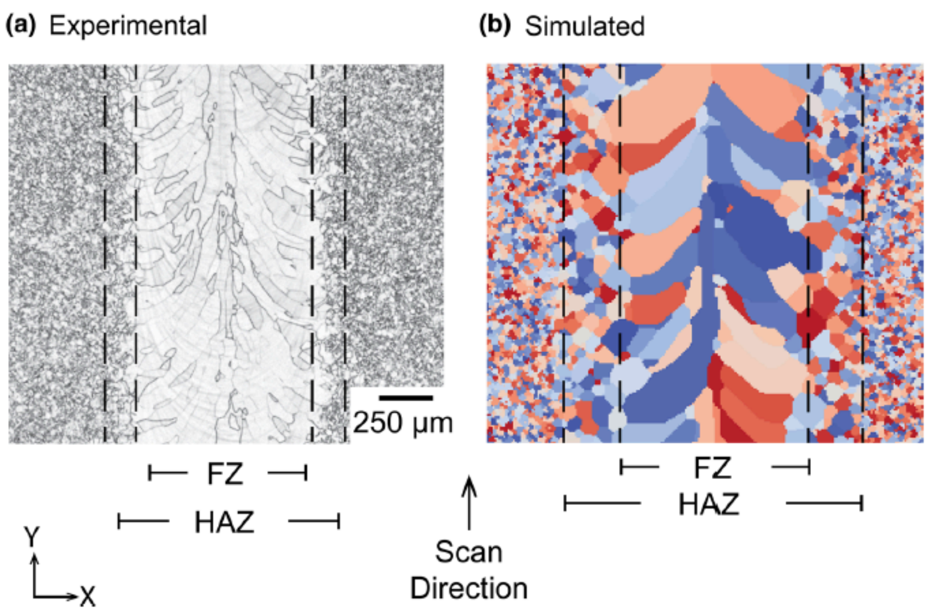

AM stress results (KMC)

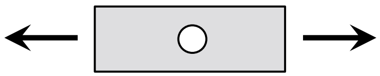

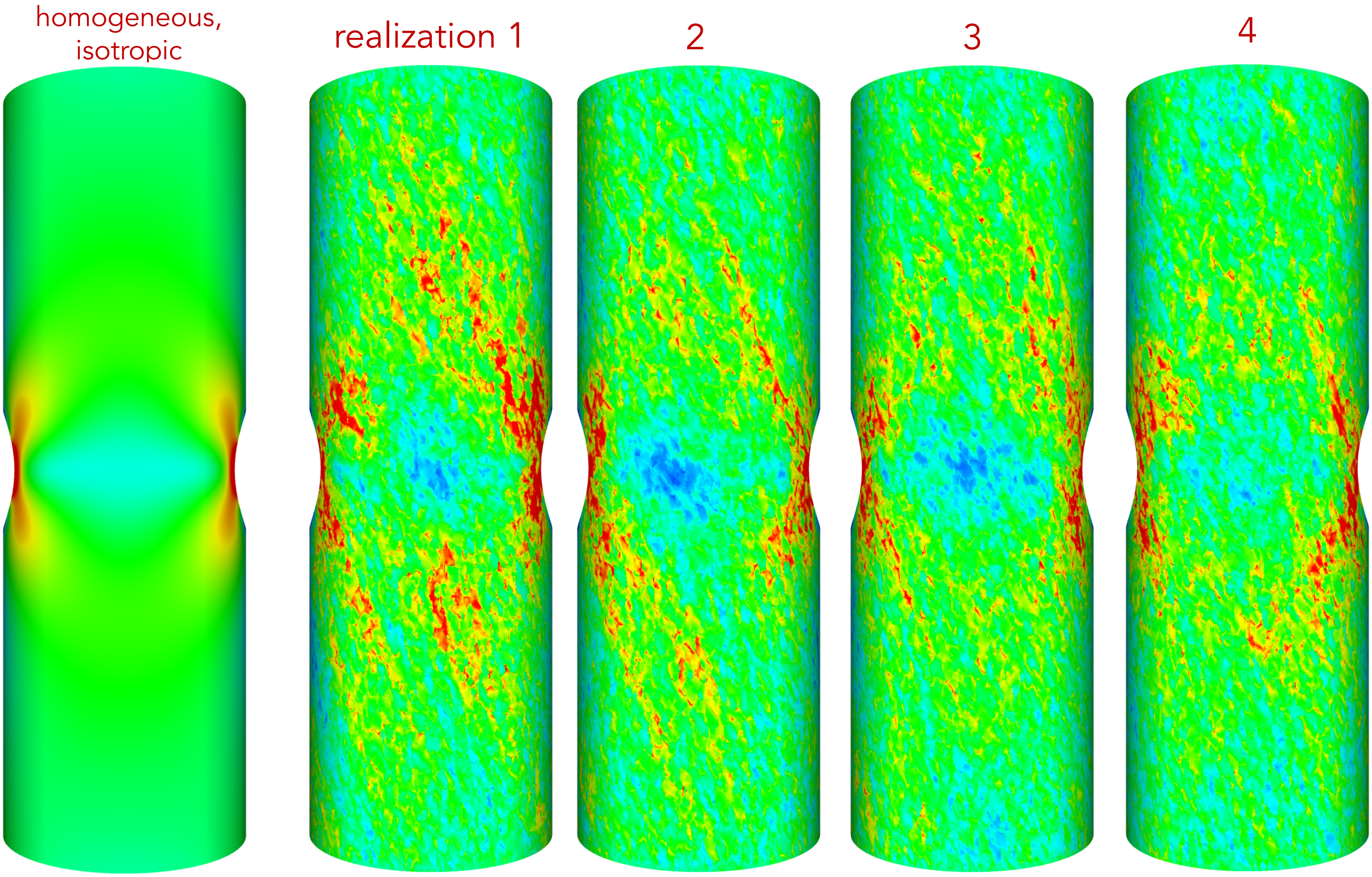

Equiaxed stress result

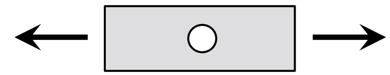

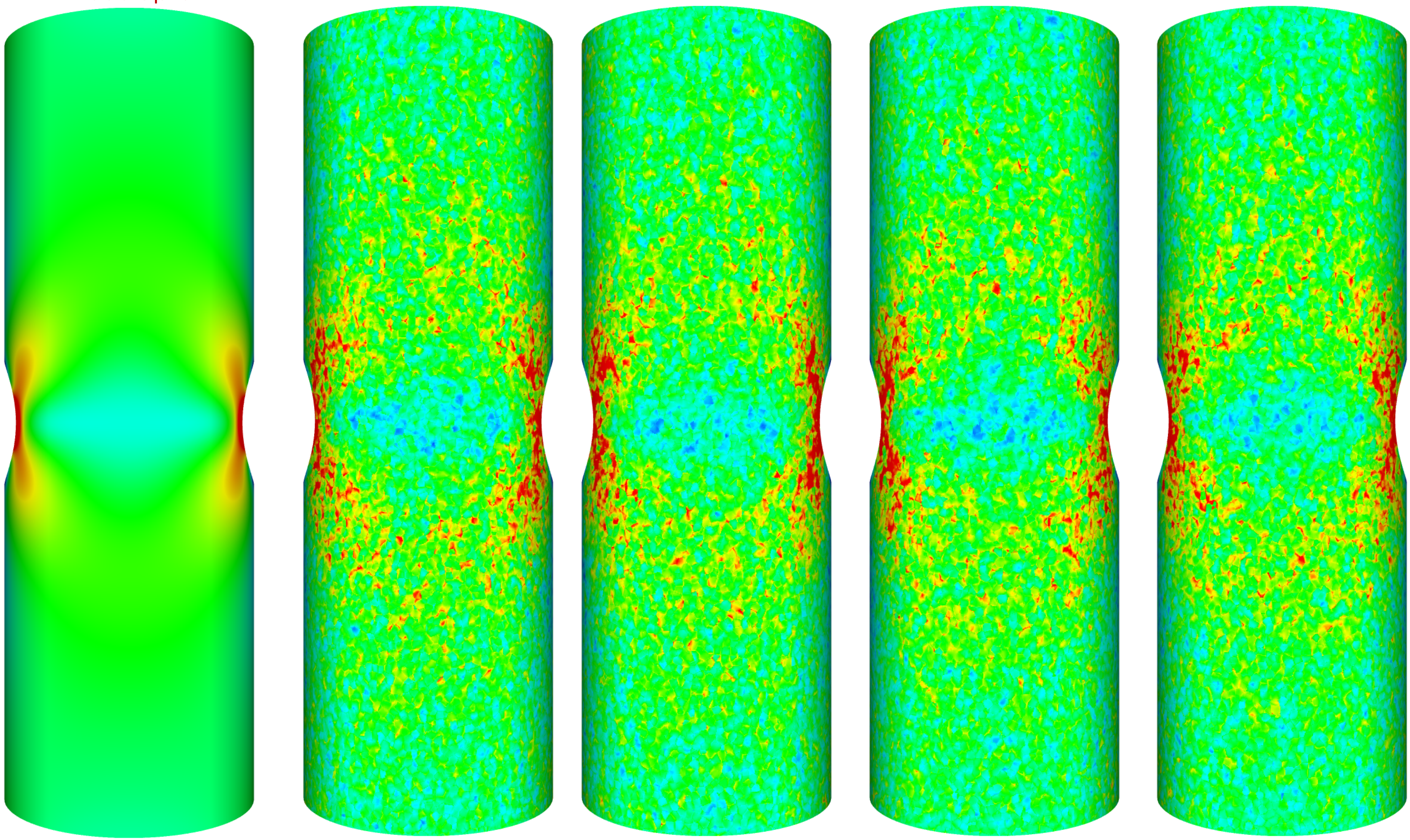

DNS vs. homogeneous

Lots of variability at microstructural scale

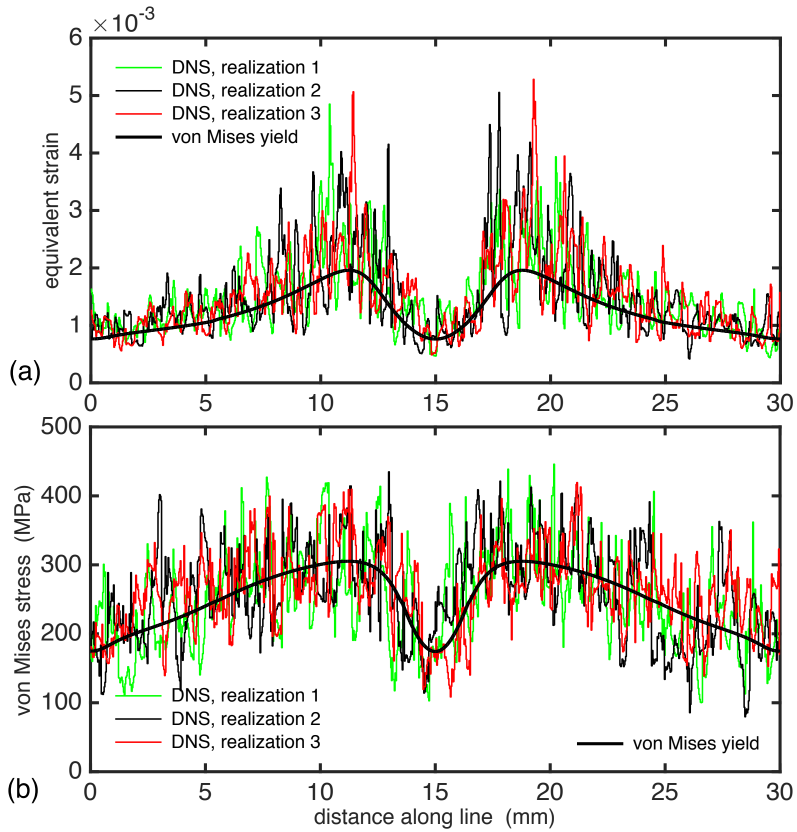

Not much variability at macroscale

Total load vs. stretch

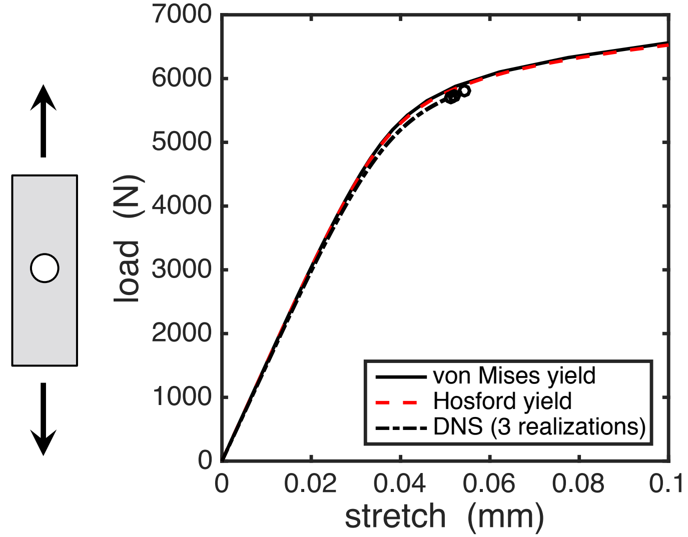

(Bishop, et. al, CMAME, 2015; Bishop, et. al, 2016, JOM)

Equiaxed
stress result

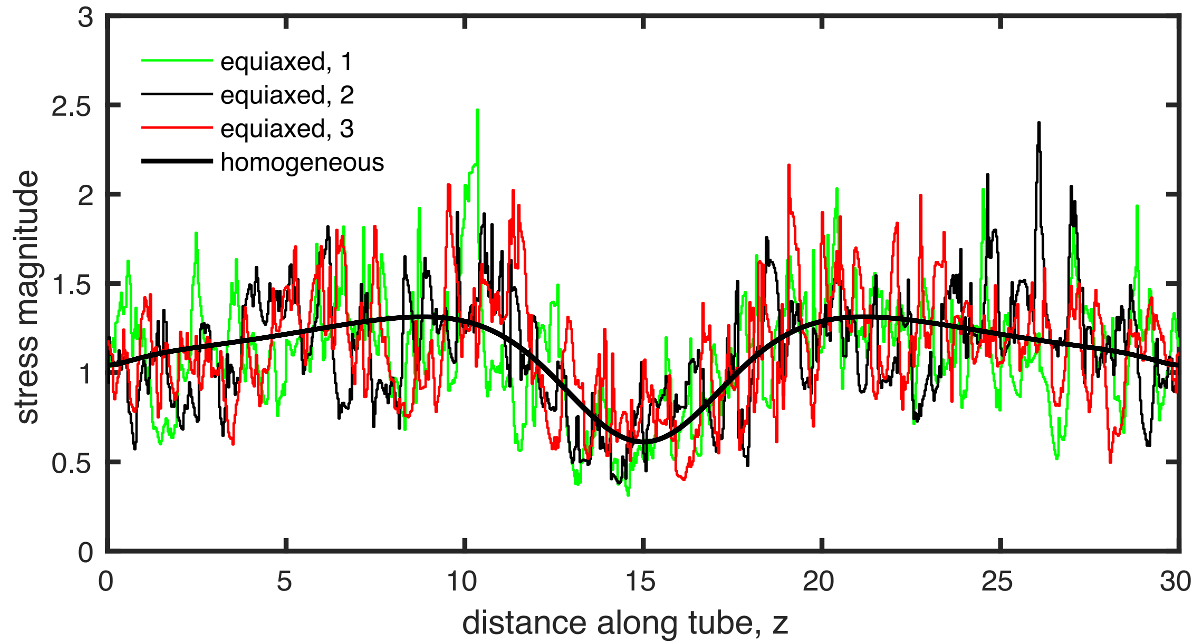

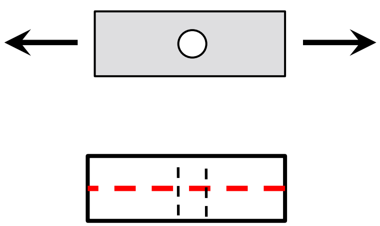

AM (KMC)
stress result

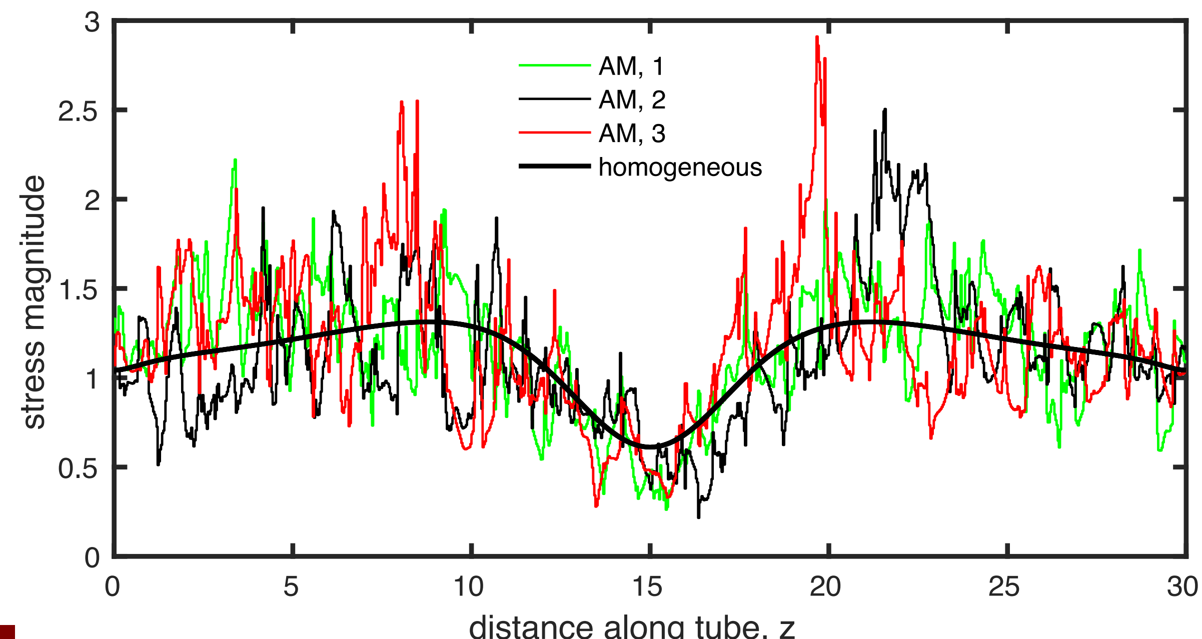

Tube stretch (elastic)

sample	equiaxed	AM	homogeneous
1	1.875	1.912	1.842
2	1.882	1.888	–
3	1.881	1.895	–
4	1.885	1.860	–
5	1.885	1.972	–
6	1.880	1.920	–
7	1.879	1.880	–
8	1.879	1.925	–
9	1.870	1.941	–
10	1.885	1.922	–
mean	1.880	1.911	1.842
sdev	0.004	0.032	0.000

cumulative distribution function

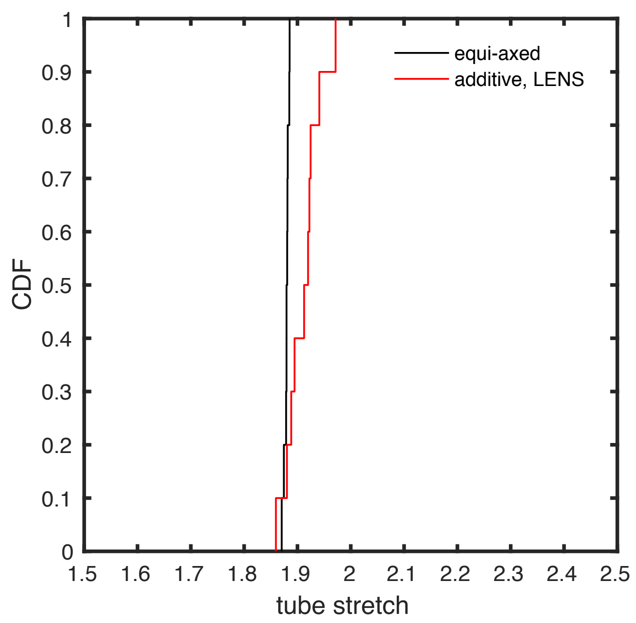

Observations

Type 1, each submodel is independent

- "embarrasingly" parallel

Type 2, each submodel overlaps

- need to use a "coloring algorithm" to sequence submodel simulations
- each color is a set of submodels
- next set uses results from previous set (color)
- this example requires 6 colors using simple "greedy" algorithm
- each set of submodels can be run independently in parallel.
- type of Schwarz iteration

$$J(\mathbf{u}^0) \geq J(\mathbf{w}_1) \geq J(\mathbf{w}_2) \geq J(\mathbf{w}_3) \ldots$$

(reduction in potential energy)